MATHEMATICS OF COMPUTATION
VOLUME 54, NUMBER 190
APRIL 1990, PAGES 545-581

THE RUNGE-KUTTA LOCAL PROJECTION DISCONTINUOUS GALERKIN FINITE ELEMENT METHOD FOR CONSERVATION LAWS IV: THE MULTIDIMENSIONAL CASE

BERNARDO COCKBURN, SUCHUNG HOU, AND CHI-WANG SHU

ABSTRACT. In this paper we study the two-dimensional version of the Runge-Kutta Local Projection Discontinuous Galerkin (RKDG) methods, already defined and analyzed in the one-dimensional case. These schemes are defined on general triangulations. They can easily handle the boundary conditions, verify maximum principles, and are formally uniformly high-order accurate. Preliminary numerical results showing the performance of the schemes on a variety of initial-boundary value problems are shown.

1. INTRODUCTION

This is the fourth article of a series in which we introduce, analyze and test numerically the RKDG methods. These new numerical methods are designed to obtain approximations of the physically relevant solution of the initial-boundary value problem associated with the hyperbolic conservation law

$$\partial_t u + \operatorname{div} \mathbf{f} = 0 \quad \text{in } (0, T) \times \Omega, \tag{1.1a}$$

where $\Omega \subset \mathbb{R}^d$, $u = (u_1, \ldots, u_m)^t$, and $\mathbf{f}$ is such that any real combination of the Jacobian matrices $\sum_{i=1}^{d} \xi_i \frac{\partial f_i}{\partial u}$ has m real eigenvalues and a complete set of eigenvectors. The case $d = 1$ has been treated in [5, 6, and 7]. In [5] the idea of the method was introduced, and the model scheme, for which the approximate solution is taken to be piecewise linear in space, was studied in the framework of periodic boundary conditions. The resulting scheme was proven to be formally uniformly of order two, and to converge to a weak solution of (1.1). Numerical results showing the uniform second-order accuracy as well as the convergence to the entropy solution in several cases were displayed. In [6] we extended these results to the general case, i.e., to the case of arbitrary boundary conditions and an approximate solution piecewise polynomial of degree k in space. A local maximum principle, the TVBM (total variation bounded in the means) and the TVB (total variation bounded) properties,

Received February 23, 1989.
1980 *Mathematics Subject Classification* (1985 *Revision*). Primary 65M60, 65N30, 35L65.
Key words and phrases. Discontinuous finite elements, local projection, multidimensional conservation laws.
The first and second authors were partially supported by a Grant of the Minnesota Supercomputer Institute. The third author was partially supported by NSF grant DMS88-10150.

0025-5718/90 $1.00 + $.25 per page

as well as convergence to a weak solution were proven. A formal uniform order of accuracy of $(k+1)$ was obtained, and was verified numerically for $k=1,2$ in several cases. Convergence to the entropy solution, as well as sharp capture of discontinuities, were also observed in these cases, even for non-convex fluxes $\mathbf{f}$. Finally, in [7] the schemes were extended to systems ($m>1$), and numerical examples (showing the good performance of the methods for $k=1,2$, and $m=2,3$) were presented. Special attention was given to the Euler equations of gas dynamics. In this paper we shall extend our schemes to the multidimensional scalar case $(m=1, d>1)$. We thus complete (1.1a) with the initial condition

$$u(t=0)=u_0 \quad \text{in } \Omega, \tag{1.1b}$$

where $u_0 \in L^\infty(\Omega)$, and the boundary condition

$$u=\gamma \quad \text{in } (0,T)\times\partial\Omega, \tag{1.1c}$$

where $\gamma \in L^\infty((0,T)\times\partial\Omega)$. See Bardos et al. [1] for a correct interpretation of this condition. For the sake of clarity we shall restrict ourselves to the two-dimensional case, $d=2$.

When passing from the one-dimensional case to the multidimensional case, the main challenge comes from the complicated geometry the domain Ω may have in practical applications. In this respect, finite element methods, such as the SUPG-method of Hughes and Brook [19, 20, 21, 22, 23, 24] (which has been analyzed by Johnson et al. in [25, 26, and 27]), are better suited than finite difference methods, like for example the current versions of the ENO schemes [17, 18, 15, 16, 38, 39], or the Bell-Dawson-Shubin scheme [2]. This is the main reason why the RKDG methods use a finite element discretization in space. The particular finite elements of our method allow an extremely simple treatment of the boundary conditions. No special numerical treatment of them is required in order to achieve uniform high-order accuracy, as is the case for the finite difference schemes.

Another challenge is given by the increase of the complexity of the structure of the discontinuities. In the one-dimensional case, the Riemann problem can be solved in closed form, and discontinuity curves in the (x,t) plane are simple straight lines passing through the origin. However, in two dimensions, only some special cases of the general Riemann problem have already been solved, and those display a very rich structure; see the works of Wagner [43], Lindquist [28, 29], and Tong et al. [41, 42]. Thus, methods which allow triangulations that can be easily adapted to resolve this structure, should seriously be taken into consideration. Our methods allow extremely general triangulations. Moreover, the degree of the polynomial defining the approximate solution can be easily changed from element to element. Thus, adaptive versions of the RKDG methods can be easily defined and shall constitute the subject of a forthcoming work.

From a theoretical point of view, the passage from $d=1$ to $d=2$ is dra-

matic. In the one-dimensional case, it is possible to devise high-order accurate schemes with the TVD (total variation diminishing) property, a property that implies the compactness of the sequence of approximate solutions generated by the schemes. (The TVD schemes were introduced by Harten [14], and a wide class of them was analyzed by Sweby [40]. Among these schemes we have, for example, (i) the MUSCL schemes, as analyzed by Osher [32], (ii) the schemes of Osher and Chakravarthy [33], (iii) the schemes obtained by a TVD time discretization introduced by Shu [37], and (iv) the quasi-monotone schemes introduced by Cockburn [8, 9, 10].) Unfortunately, in two dimensions, any TVD scheme is at most first-order accurate. This interesting result was proven by Goodman and LeVeque [13]. In [10] it is shown under which conditions a quasi-monotone scheme (which is TVD) is formally high-order accurate in two dimensions, but these conditions are quite restrictive. Thus, for $d = 2$, there is a strong incompatibility between TVD compactness and high-order accuracy. We must emphasize, however, that even in the one-dimensional case these two properties are in conflict, for TVD schemes cannot be uniformly high-order accurate: they are at most first-order accurate at the critical points of the exact solution. This difficulty prompted the appearance of the so-called TVB (total variation bounded) schemes, which came out from rather different approaches. (Lucier [30] introduced a semidiscrete TVB scheme for which he proved an $L^{\infty}(0, T; L^{1})$ rate of convergence of $O(N^{-2})$, where N is the number of degrees of freedom defining the approximate solution. This result is true even if the exact solution has a finite number of discontinuities, a very surprising result that is now leading to even more surprising regularity results for the continuous problem; see [31]. Shu [35, 36], introduced a general technique to obtain uniformly high-order accurate TVB schemes starting from TVD schemes; Sanders [34] introduced a third-order accurate TVB scheme (which is TVD under another definition of total variation) whose accuracy degenerates to second order at critical points; the RKDG schemes are TVB schemes which are uniformly kth-order accurate, $k \geq 1$, [5, 6, 7].) However, to prove the TVB property in two dimensions is a rather difficult task, even for the simplest monotone scheme, if arbitrary triangulations are considered. On the other hand, maximum principles are not incompatible with high-order accuracy, but it is well known that L^{∞} boundedness does not allow us to pass to the limit in the nonlinearity. Some kind of workable compactness criterion, one between TVB compactness and L^{∞} boundedness, which is not in conflict with high-order accuracy, is still to be discovered and seems to be an interesting and challenging problem. Meanwhile, we shall content ourselves in obtaining maximum principles for the RKDG methods, a very desirable property in this kind of problems in which the values of the solution u have physical meaning only in determined intervals. We remark that to the knowledge of the authors, no other class of schemes has a proven maximum principle for general nonlinearities $\mathbf{f}$, and arbitrary triangulations.

An outline of the paper follows. In §2 we present and analyze our schemes.

The main result is the definition of the local projection $\Lambda\Pi$ for arbitrary triangulations, which does not destroy the high-order accuracy of the scheme while enforcing a local maximum principle *and* allowing an extremely simple treatment of the boundary conditions. In §3 we present several numerical results, and in §4 we end with a summary and some concluding remarks.

2. General formulation

2.1. Preliminaries and notations. Let $\{t^n\}_{n=0}^{nt}$ be a partition of $[0, T]$. Set, as usual, $\Delta t^n = t^{n+1} - t^n$, $n = 0, \dots, nt - 1$. Let us assume that the domain Ω is polygonal, and let us denote by $\mathcal{T}_h$ a triangulation of Ω. For the sake of simplicity we assume that if two elements of $\mathcal{T}_h$, say K_1 and K_2, are such that $e = K_1 \cap K_2 \neq \varnothing$, then e is either an edge of both K_1 and K_2 or a point.

We shall denote by V_h the space of elements of $L^\infty(\Omega)$ whose restriction to $K \in \mathcal{T}_h$ belongs to a vector space $V(K)$. Note that the space $V(K)$ may be different for different elements K. The triangulation $\mathcal{T}_h$ of Ω induces a triangulation of $\partial\Omega$ that we shall denote by $\partial\mathcal{T}_h$. Let us denote by ∂V_h the space of functions of $L^\infty(\partial\Omega)$ which are traces of functions of $V_h(\Omega)$.

As stated in [5, 6, and 7], to construct the RKDG methods, we proceed as follows. First we discretize (1.1) in space using the Discontinuous Galerkin Method. The resulting equation can be put in ODE form as $\frac{d}{dt}u_h = L_h(u_h, \gamma_h(t))$. Then, this ODE is discretized in time using the TVD Runge-Kutta time discretization introduced in [38]. Finally, a local projection $\Lambda\Pi_h$ is applied to the intermediate values of the Runge-Kutta discretization, in order to enforce stability. The general RKDG method then has the following form [7]:

(2.1a) Set $u_h^0 = \Lambda\Pi_h \, \mathbb{P}_{V_h}(u_0)$;

(2.1b) For $n = 0, \dots, nt - 1$ compute u_h^{n+1} as follows:

(i) set $u_h^{(0)} = u_h^n$;

(ii) for $i = 1, \dots, k + 1$ compute the intermediate functions:

$$u_h^{(i)} = \Lambda\Pi_h \left\{ \sum_{l=0}^{i-1} [\alpha_{il} u_h^{(l)} + \beta_{il} \Delta t^n L_h(u_h^{(l)}, \gamma_h(t^n + d_l \Delta t^n))] \right\};$$

(iii) set $u_h^{n+1} = u_h^{(k+1)}$;

where $\mathbb{P}_{V_h}$ is the L^2 projection into V_h, and γ_h is the L^2 projection of γ into ∂V_h. Note that this method is easy to code, for only a subroutine defining $L_h(u_h, \gamma_h(t))$, and one defining $\Lambda\Pi_h$, are needed. Some Runge-Kutta time discretization parameters are displayed in the table below, see [39].

In what follows we shall first describe in detail the operator L_h. Then we shall obtain conditions under which the RKDG methods satisfy maximum principles. The local projection $\Lambda\Pi_h$ will then be constructed in order to enforce those conditions. The stability and convergence properties of these schemes are summarized at the end of this section.

TABLE 1

Parameters of some practical Runge-Kutta time discretizations				
order	α_{il}	β_{il}	d_l	$\max\{\beta_{il}/\alpha_{il}\}$
2	1 $\frac{1}{2}\ \frac{1}{2}$	1 $0\ \frac{1}{2}$	0 1	1
3	1 $\frac{3}{4}\ \frac{1}{4}$ $\frac{1}{3}\ 0\ \frac{2}{3}$	1 $0\ \frac{1}{4}$ $0\ 0\ \frac{2}{3}$	0 1 $\frac{1}{2}$	1

2.2. The operator L_h. In order to determine this operator, we multiply (1.1a) by $v_h \in V_h$, integrate over $K \in \mathcal{T}_h$, and replace the exact solution u by its approximation $u_h \in V_h$:

$$\frac{d}{dt}\int_K u_h(t,x)\,v_h(x)\,dx + \int_K \operatorname{div}\mathbf{f}(u_h(t,x))\,v_h(x)\,dx = 0, \quad \forall v_h \in V_h.$$

Integrating by parts formally, we obtain

$$\frac{d}{dt}\int_K u_h(t,x)\,v_h(x)\,dx + \sum_{e\in\partial K}\int_e \mathbf{f}(u_h(t,x))\cdot\mathbf{n}_{e,K}\,v_h(x)\,d\Gamma - \int_K \mathbf{f}(u_h(t,x))\cdot\mathbf{grad}\,v_h(x)\,dx = 0, \quad \forall v_h \in V_h,$$

where $\mathbf{n}_{e,K}$ is the outward unit normal to the edge e. Notice that $\mathbf{f}(u_h(t,x))\cdot\mathbf{n}_{e,K}$ does not have a precise meaning, for u_h is discontinuous at $x \in e \in \partial K$. Thus, as in the one-dimensional case, we replace $\mathbf{f}(u_h(t,x))\cdot\mathbf{n}_{e,K}$ by the function $h_{e,K}(u_h(t,x^{\mathrm{int}(K)}), u_h(t,x^{ext(K)}))$, where

$$u_h(t,x^{\mathrm{int}(K)}) = \lim_{\substack{y\to x\\ y\in\mathring{K}}} u_h(t,y),$$

$$u_h(t,x^{\mathrm{ext}(K)}) = \begin{cases} \gamma_h(x,t) & \text{if } x\in\partial\Omega,\\ \lim\limits_{\substack{y\to x\\ y\in(K)^c}} u_h(t,y) & \text{otherwise.}\end{cases}$$

The function $h_{e,K}(\cdot,\cdot)$ is any function satisfying the following conditions:

(2.2a) $h_{e,K}(u,u) = \mathbf{f}(u)\cdot\mathbf{n}_{e,K}$,

(2.2b) $h_{e,K}(u,v)$ is nondecreasing in u and nonincreasing in v,

(2.2c) $h_{e,K}(\cdot,\cdot)$ is (globally) Lipschitz,

(2.2d)

$$h_{e,K}(u_h(t,x^{\mathrm{int}(K)}), u_h(t,x^{\mathrm{ext}(K)})) = -h_{e,K'}(u_h(t,x^{\mathrm{int}(K')}), u_h(t,x^{\mathrm{ext}(K')})), \qquad K'\cap K = e,$$

i.e., it is a consistent two-point monotone Lipschitz flux, as defined in [11], consistent with $\mathbf{f}(u)\cdot\mathbf{n}_{e,K}$. The last property justifies $h_{e,K}(\cdot,\cdot)$ as a flux. Examples of $h_{e,K}$ can be found in [7, Remark 2.4]. Sometimes we shall write simply $h_{e,K}(t,x)$ instead of $h_{e,K}(u_h(t,x^{\mathrm{int}(K)}),u_h(t,x^{\mathrm{ext}(K)}))$.

In this way we obtain

$$\frac{d}{dt}\int_K u_h(t,x)v_h(x)\,dx+\sum_{e\in\partial K}\int_e h_{e,K}(t,x)\,v_h(x)\,d\Gamma - \int_K \mathbf{f}(u_h(t,x))\cdot\mathbf{grad}\,v_h(x)\,dx=0,\quad \forall\, v_h\in V_h.$$

Of course, we have to replace the integrals by quadrature rules that we shall choose as follows:

$$\int_e h_{e,K}(t,x)\,v_h(x)\,d\Gamma\approx\sum_{l=1}^{L}\omega_l\,h_{e,K}(t,x_{el})\,v(x_{el})|e|, \tag{2.3a}$$

$$\int_K \mathbf{f}(u_h(t,x))\cdot\mathbf{grad}\,v_h(x)\,dx\approx\sum_{j=1}^{M}\underline{\omega}_j\,\mathbf{f}(u_h(t,x_{Kj}))\cdot\mathbf{grad}\,v_h(x_{Kj})|K|. \tag{2.3b}$$

Thus, we finally obtain the weak formulation:

$$\frac{d}{dt}\int_k u_h(t,x)v_h(x)\,dx+\sum_{e\in\partial K}\sum_{l=1}^{L}\omega_l\,h_{e,K}(t,x_{el})\,v(x_{el})|e| - \sum_{j=1}^{M}\underline{\omega}_j\,\mathbf{f}(u_h(t,x_{Kj}))\cdot\mathbf{grad}v_h(x_{Kj})|K|=0,\quad \forall v_h\in V_h,\quad \forall K\in\mathscr{T}_h. \tag{2.4}$$

These equations can be rewritten in ODE form as $\frac{d}{dt}u_h=L_h(u_h,\gamma_h)$, where

$$L_h:\mathscr{V}_h\times\partial\mathscr{V}_h\longrightarrow V_h, \tag{2.5a}$$

$$\frac{d}{dt}(u_h(t),v_h)=(L_h(u_h,\gamma_h),v_h),\quad \forall v_h\in V_h,\quad t\in(0,T), \tag{2.5b}$$

where $\mathscr{V}_h=\{w:\Omega\to\mathbb{R}:w|_K\in\mathscr{C}^0(K),\quad\forall K\in\mathscr{T}_h\}$, $\partial\mathscr{V}_h=\{w:\partial\Omega\to\mathbb{R}:w|_e\in\mathscr{C}^0(e),\quad\forall e\in\partial\mathscr{T}_h\}$, and $(\cdot,\cdot)$ is the usual $L^2(\Omega)$ inner product. Notice that in order to go from the weak form (2.4) to the ODE (2.5b), a matrix has to be inverted. However, this can be easily done by hand, for its order is equal to the dimension of the local space $V(K)$. It is also important to remark that any choice of the degrees of freedom of the approximate solution is allowed in this formulation.

Thus, the operator $L_h(u_h,\gamma_h)$ is a discrete approximation of $-\mathrm{div}\,\mathbf{f}(u)$ (together with the corresponding boundary conditions!). The following result gives an indication of the quality of this approximation.

Proposition 2.1. *Let* $\mathbf{f}(u) \in W^{k+2,\infty}(\Omega)$, *and set* $\gamma = \text{trace}(u)$. *Let the quadrature rule over the edges be exact for polynomials of degree* $(2k+1)$, *and let the one over the element be exact for polynomials of degree* $(2k)$. *Assume that the family of triangulations* $\mathcal{F} = \{\mathcal{T}_h\}_{h>0}$ *is regular, i.e., that there is a constant* σ *such that*

$$\frac{h_K}{\rho_K} \geq \sigma, \quad \forall K \in \mathcal{T}_h, \quad \forall \mathcal{T}_h \in \mathcal{F}, \tag{2.6}$$

where h_K *is the diameter of* K, *and* ρ_K *is the diameter of the biggest ball included in* K. *Then, if* $V(K) \supset P^k(K), \quad \forall K \in \mathcal{T}_h$:

$$\|L_h(u, \gamma) + \operatorname{div} \mathbf{f}(u)\|_{L^\infty(\Omega)} \leq C h^{k+1} |\mathbf{f}(u)|_{W^{k+2,\infty}(\Omega)}.$$

We are, of course, assuming implicitly that the dimension of the local space $V(K)$ is uniformly bounded from above. A p-version of these schemes can certainly be considered, but we shall leave this as the subject of future work.

For the proof we shall need the following direct consequence of the Bramble-Hilbert Lemma, [4, Theorem 4.1.3].

Lemma 2.2. *Let* $E_\Omega(\phi) = \int_\Omega \phi - \sum_{l=1}^{L} \omega_l \phi(x_l) |\Omega|$, *and suppose that* $E_\Omega(\phi) = 0, \ \forall \phi \in P^r(\Omega)$. *Then,*

$$|E_\Omega(g\psi)| \leq C|\Omega| h^{r+1-s} |\psi|_{L^\infty(\Omega)} |g|_{W^{r+1-s,\infty}(\Omega)}, \quad \forall \psi \in P^s(\Omega),$$

where $h = \operatorname{diam} \Omega$.

Proof (of Proposition 2.1). We have

$$\|L_h(u, \gamma) + \operatorname{div} \mathbf{f}(u)\|_{L^\infty(K)} \leq e_1 + e_2,$$

where

$$e_1 = \|\operatorname{div} \mathbf{f}(u) - \mathbb{P}_{P^k(K)}(\operatorname{div} \mathbf{f}(u))\|_{L^\infty(K)},$$
$$e_2 = \|L_h(u, \gamma) + \mathbb{P}_{P^k(K)}(\operatorname{div} \mathbf{f}(u))\|_{L^\infty(K)},$$

and $\mathbb{P}_{P^k(K)}$ is the L^2 projection into $P^k(K)$. Using the regularity of the triangulation $\mathcal{T}_h$, we obtain by a well-known approximation theory result, [4, Theorem 3.1.6], that:

$$e_1 \leq C\, h^{k+1} |\operatorname{div} \mathbf{f}(u)|_{W(K)^{k+1,\infty}}.$$

To estimate e_2, we proceed as follows. Taking into account the definition of L_h, (2.5), (2.4), we have, for $v_h \in P^k(K)$,

$$\begin{aligned}
\Theta(v_h) &= \frac{1}{|K|}\int_K (L_h(u,\gamma) + \mathbb{P}_{P^k(K)}(\operatorname{div}\mathbf{f}(u)))\, v_h\, dx \\
&= \frac{1}{|K|}\int_K (L_h(u,\gamma) + \operatorname{div}\mathbf{f}(u)) v_h\, dx \\
&= \frac{1}{|K|}\int_K L_h(u,\gamma)\, v_h\, dx \\
&\quad + \frac{1}{|K|}\sum_{e\in\partial K}\int_e \mathbf{f}(u(t,x))\cdot\mathbf{n}_{e,K}\, v_h(x)\, d\Gamma \\
&\quad - \frac{1}{|K|}\int_K \mathbf{f}(u_h(x,t))\cdot\mathbf{grad}\, v_h(x)\, dx \\
&= \frac{1}{|K|}\sum_{e\in\partial K} E_e(\mathbf{f}(u)\cdot\mathbf{n}_{e,K}\, v_h) - \frac{1}{|K|}E_K(\mathbf{f}(u)\cdot\mathbf{grad} v_h),
\end{aligned}$$

where

$$\begin{aligned}
E_e(\phi) &= \int_e \phi - \sum_{i=1}^{L}\omega_i\phi(x_{ei})|e|\ , \\
E_K(\phi) &= \int_K \phi - \sum_{j=1}^{M}\underline{\omega}_j\phi(x_{Kj})\ |K|.
\end{aligned}$$

But,

$$\begin{aligned}
\frac{1}{|K|}|E_e(\mathbf{f}(u)\cdot\mathbf{n}_{e,K}\, v_h)| &\le C\frac{|e|}{|K|}h^{k+2}|\mathbf{f}(u)\cdot\mathbf{n}_{e,K}|_{W^{k+2,\infty}(e)}|v_h|_{L^\infty(K)}, \\
&\qquad \text{by hypothesis and Lemma 2.2,} \\
&\le Ch^{k+1}|\mathbf{f}(u)|_{W^{k+2,\infty}(K)}|v_h|_{L^\infty(K)}, \\
&\qquad \text{by the regularity of the triangulation,}
\end{aligned}$$

and similarly,

$$\frac{1}{|K|}|E_K(\mathbf{f}(u)\cdot\mathbf{grad} v_h)| \le Ch^{k+1}|\mathbf{f}(u)|_{W^{k+2,\infty}(K)}|v_h|_{L^\infty(K)}.$$

The result follows by setting $v_h = L_h(u,\gamma) + \mathbb{P}_{V_h}(\operatorname{div}\mathbf{f}(u))$ and using the inequality

$$|w_h|^2_{L^\infty(K)} \le C\frac{1}{|K|}|w_h|^2_{L^2(K)},$$

which is valid if $w_h \in V(K)$. (Notice that all the norms are equivalent in finite-dimensional spaces; the factor $1/|K|$ follows from a standard scaling argument,

see [4, (3.2.24)].) The constant C depends solely on the dimension of $V(K)$, which was implicitly assumed to be uniformly bounded. □

2.3. In quest of a maximum principle. We now consider the problem of rendering our schemes L^∞ stable. As we said earlier, we shall construct a local projection $\Lambda\Pi_h$ whose task will be to enforce a maximum principle on them. The fact that this is indeed possible is to a great extent due to the form of the time discretization technique, as we show below. Let us write u_h as $\overline{u}_h + \tilde{u}_h$, where $\overline{u}_h$ is piecewise constant and $\tilde{u}_h$ has zero mean in each element K. The restriction of $\overline{u}_h$ to the element K will be denoted by $\overline{u}_K$.

Lemma 2.3. *Let the coefficients α_{il} of the Runge-Kutta time discretization be positive and such that $\sum_{l=0}^{i-1} \alpha_{il} = 1$ for $i = 1, \dots, k+1$. Set $w_h = u_h + \delta \Delta t^m L_h(u_h, \gamma_h)$, and suppose that for $cfl \in [0, cfl_0/|\delta|]$, where*

$$cfl = \sup_{n=1,\cdots,nt;\, e\in\partial K;\, K\in\mathcal{T}_h} \Delta t^n \frac{|e|}{|K|} \|\mathbf{f}' \cdot \mathbf{n}_{e,K}\|_{L^\infty[a_0,b_0]}, \tag{2.7a}$$

$$a_0 = \inf_{x\in\Omega,\, t\in(0,t^{n+1}),\, y\in\partial\Omega} \{u_0(x), \gamma(t,y)\}, \tag{2.7b}$$

$$b_0 = \sup_{x\in\Omega,\, t\in(0,t^{n+1}),\, y\in\partial\Omega} \{u_0(x), \gamma(t,y)\}, \tag{2.7c}$$

the following maximum principle is verified:

$$\overline{u}_h, \gamma_h \in [a, b] \Rightarrow \overline{w}_h \in [a - Mh^2, b + Mh^2], \tag{2.8}$$

where M is some nonnegative parameter. Then, if $cfl \in [0, cfl_0/|\max_{i,l}\{|\frac{\beta_{il}}{\alpha_{il}}\}|]$,

$$\overline{u}_h^n \in [a_0 - (k+1)nMh^2, b_0 + (k+1)nMh^2].$$

Proof. We proceed by induction. Assume that

$$\overline{u}_h^m \in [a_0 - (k+1)mMh^2, b_0 + (k+1)mMh^2] \quad \text{for } m = 0, \dots, n.$$

The case $m = 0$ is trivially verified. Let us prove that the same is true for $m = n+1$. Set $[a, b] = [a_0 - (k+1)nMh^2, b_0 + (k+1)nMh^2]$. We claim that $\overline{u}_h^{(l)} \in [a - lMh^2, b + lMh^2]$ for $l = 0, \dots, k+1$. This is true for $l = 0$, for $u_h^{(0)} = u_h^n$ by (2.1b) (i). Assume it is true for $l = 0, \dots, i-1$. Then, by the definition (2.1b) of the intermediate function $u_h^{(i)}$:

$$\begin{aligned} u_h^{(i)} &= \sum_{l=0}^{i-1} [\alpha_{il} u_h^{(l)} + \beta_{il} \Delta t^n L_h(u_h^{(l)}, \gamma_h(t^n + d_l \Delta t^n))] \\ &= \sum_{l=0}^{i-1} \alpha_{il} \left\{ u_h^{(l)} + \frac{\beta_{il}}{\alpha_{il}} \Delta t^n L_h(u_h^{(l)}, \gamma_h(t^n + d_l \Delta t^n)) \right\}. \end{aligned}$$

This implies, using (2.8), that

$$\begin{aligned}\overline{u}_h^{(i)} &\in \sum_{l=0}^{i-1} \alpha_{il}[a-(l+1)Mh^2,\, b+(l+1)Mh^2] \\ &\subset \left\{\sum_{l=0}^{i-1} \alpha_{il}\right\}[a-iMh^2,\, b+iMh^2] \\ &= [a-iMh^2,\, b+iMh^2].\end{aligned}$$

But, by (2.1b)(iii), $u_h^{n+1} = u_h^{(k+1)}$, and so $\overline{u}_h^{n+1} = \overline{u}_h^{(k+1)} \in [a-(k+1)Mh^2,\, b+(k+1)Mh^2]$. This completes the proof. □

In this way, the existence of a maximum principle for the RKGD schemes is reduced to the existence of the maximum principle (2.8). Thus, to construct the projection $\Lambda\Pi_h$, we first study the conditions (on u_h) under which the maximum principle (2.8) holds, and then we define $\Lambda\Pi_h$ in order to enforce them. This is the approach we took in the one-dimensional scalar case, and is the same we shall take in this case. Next, we study those conditions. The actual construction of $\Lambda\Pi_h$ will be considered in the next section.

If $e \in \partial K$, let us denote by K_e the element such that $K \cap K_e = e$. In this way, if x_{el} is the lth point of the quadrature rule (2.3a) on the edge e, we shall write

$$\begin{aligned}u_h(x_{el}^{\mathrm{int}(K)}) &= u_{K,el} = \overline{u}_K + \tilde{u}_{K,el}, \\ u_h(x_{el}^{\mathrm{ext}(K)}) &= u_{K_e,el} = \overline{u}_{K_e} + \tilde{u}_{K_e,el}, \\ \gamma_h(x_{el}) &= \gamma_{el}.\end{aligned}$$

Set $w_h = u_h + \delta' L_h(u_h, \gamma_h)$, where $\delta' = \Delta t^m \cdot \delta$. Thus, by the definition of $L_h(u_h, \gamma_h)$, (2.4), (2,5):

$$\begin{aligned}\overline{w}_K = \overline{u}_K &- \left\{\sum_{e\in\partial K\setminus\partial\Omega}\sum_{l=1}^{L}\left[\frac{\delta'\omega_l|e|}{|K|}\right] h_{e,K}(u_{K,el}, u_{K_e,el})\right\} \\ &- \left\{\sum_{e\in\partial K\cap\partial\Omega}\sum_{l=1}^{L}\left[\frac{\delta'\omega_l|e|}{|K|}\right] h_{e,K}(u_{K,el}, \gamma_{el})\right\}.\end{aligned}$$

Noting that

$$\sum_{e\in\partial K}\sum_{l=1}^{L}\left[\frac{\delta'\omega_l|e|}{|K|}\right] h_{e,K}(\overline{u}_K, \overline{u}_K) = \frac{\delta'}{|K|}\int_{\partial K} \mathbf{f}(\overline{u}_K)\cdot\mathbf{n} = 0,$$

we can write

$$\begin{aligned}
\overline{w}_K &= \overline{u}_K - \left\{ \sum_{e\in\partial K\setminus\partial\Omega} \sum_{l=1}^{L} \left[\frac{\delta' \omega_l |e|}{|K|} \right] (h_{e,K}(u_{K,el}, u_{K_e,el}) - h_{e,K}(\overline{u}_K, \overline{u}_K)) \right\} \\
&\quad - \left\{ \sum_{e\in\partial K\cap\partial\Omega} \sum_{l=1}^{L} \left[\frac{\delta' \omega_l |e|}{|K|} \right] (h_{e,K}(u_{K,el}, \gamma_{el}) - h_{e,K}(\overline{u}_K, \overline{u}_K)) \right\} \\
&= \overline{u}_K - \left\{ \sum_{e\in\partial K\setminus\partial\Omega} \sum_{l=1}^{L} \left[\frac{\delta' \omega_l |e|}{|K|} \right] \{(h_{e,K}(u_{K,el}, u_{K_e,el}) - h_{e,K}(\overline{u}_K, u_{K_e,el})) \right. \\
&\qquad \left. + (h_{e,K}(\overline{u}_K, u_{K_e,el}) - h_{e,K}(\overline{u}_K, \overline{u}_K))\} \right\} \\
&\quad - \left\{ \sum_{e\in\partial K\cap\partial\Omega} \sum_{l=1}^{L} \left[\frac{\delta' \omega_l |e|}{|K|} \right] \{(h_{e,K}(u_{K,el}, \gamma_{el}) - h_{e,K}(\overline{u}_K, \gamma_{el})) \right. \\
&\qquad \left. + (h_{e,K}(\overline{u}_K, \gamma_{el}) - h_{e,K}(\overline{u}_K, \overline{u}_K))\} \right\}.
\end{aligned}$$

Using the fact that the one-dimensional flux $h_{e,K}$ is Lipschitz, we obtain

$$\begin{aligned}
\overline{w}_K &= \overline{u}_K - \left\{ \sum_{e\in\partial K\setminus\partial\Omega} \sum_{l=1}^{L} \left[\frac{\delta' \omega_l |e|}{|K|} \right] \{h_{el,1}\{\tilde{u}_{K,el}\} \right. \\
&\qquad \left. + h_{el,2}(\{\overline{u}_{K_e} - \overline{u}_K\} + \{\tilde{u}_{K_e,el}\})\} \right\} \\
&\quad - \left\{ \sum_{e\in\partial K\cap\partial\Omega} \sum_{l=1}^{L} \left[\frac{\delta' \omega_l |e|}{|K|} \right] \{h_{el,1}\{\tilde{u}_{K,el}\} + h_{el,2}(\{\gamma_{el} - \overline{u}_K\})\} \right\} \\
&= \overline{u}_K + \left\{ \sum_{e\in\partial K\setminus\partial\Omega} \sum_{l=1}^{L} \left[-\frac{\delta' \omega_l |e|}{|K|} h_{el,2} \right] \{\overline{u}_{K_e} - \overline{u}_K\} \right. \\
&\qquad \left. + \sum_{e\in\partial K\cap\partial\Omega} \sum_{l=1}^{L} \left[-\frac{\delta' \omega_l |e|}{|K|} h_{el,2} \right] \{\gamma_{el} - \overline{u}_K\} \right\} \\
&\quad + \left\{ \sum_{e\in\partial K} \sum_{l=1}^{L} \left[\frac{\delta' \omega_l |e|}{|K|} h_{el,1} \right] \{-\tilde{u}_{K,el}\} \right. \\
&\qquad \left. + \sum_{e\in\partial K\setminus\partial\Omega} \sum_{l=1}^{L} \left[-\frac{\delta' \omega_l |e|}{|K|} h_{el,2} \right] \{\tilde{u}_{K_e,el}\} \right\}.
\end{aligned}$$

If we assume that $\omega_l \geq 0$, then the quantities between brackets are nonnegative numbers, by (2.2b), which are bounded from above, thanks to (2.2c). Now, if the quantities $-\tilde{u}_{K,el}$ and $\tilde{u}_{K_e,el}$ can be written as positive linear combinations

of $\overline{u}_{K_e} - \overline{u}_K$, and $\overline{\gamma}_e - \overline{u}_K$, i.e., if

$$-\tilde{u}_{K,el} = \sum_{d\in\partial K\setminus\partial\Omega} \theta_{K,eld}(\overline{u}_{K_d} - \overline{u}_K) + \sum_{d\in\partial K\cap\partial\Omega} \theta_{K,eld}(\overline{\gamma}_d - \overline{u}_K), \tag{2.9a}$$

$$\tilde{u}_{K_e,el} = \sum_{d\in\partial K\setminus\partial\Omega} \eta_{K_e,eld}(\overline{u}_{K_d} - \overline{u}_K) + \sum_{d\in\partial K\cap\partial\Omega} \eta_{K_e,eld}(\overline{\gamma}_d - \overline{u}_K), \tag{2.9b}$$

where

$$\theta_{K,eld},\ \eta_{K_e,eld} \geq 0, \tag{2.9c}$$

and

$$\overline{\gamma}_e = \sum_{l=1}^{L} \omega_l\, \gamma_{el}, \tag{2.9d}$$

then

$$\overline{w}_K = \overline{u}_K + \delta\Delta t^m \cdot \left\{ \sum_{e\in\partial K\setminus\partial\Omega} \Theta_e\{\overline{u}_{K_e} - \overline{u}_K\} + \sum_{e\in\partial K\cap\partial\Omega} \sum_{l=1}^{L} \Theta_{el}(\gamma_{el} - \overline{u}_K) \right\},$$

where

$$\begin{aligned}\Theta_e = \sum_{l=1}^{L} \frac{\omega_l|e|}{|K|}[-h_{el,2}] &+ \sum_{d\in\partial K} \sum_{l=1}^{L} \frac{\omega_l|d|}{|K|}[h_{dl,1}]\theta_{K,dle} \\ &+ \sum_{d\in\partial K\setminus\partial\Omega} \sum_{l=1}^{L} \frac{\omega_l|d|}{|K|}[-h_{dl,2}]\eta_{K_d,dle},\end{aligned} \tag{2.10a}$$

$$\begin{aligned}\Theta_{el} = \frac{\omega_l|e|}{|K|}[-h_{el,2}] &+ \omega_l \sum_{d\in\partial K} \sum_{l=1}^{L} \frac{\omega_l|d|}{|K|}[h_{dl,1}]\theta_{K,dle} \\ &+ \omega_l \sum_{d\in\partial K\setminus\partial\Omega} \sum_{l=1}^{L} \frac{\omega_l|d|}{|K|}[-h_{dl,2}]\eta_{K_d,dle}.\end{aligned} \tag{2.10b}$$

Thus, if

$$\sum_{e\in\partial K\setminus\partial\Omega} \Theta_e + \sum_{e\in\partial K\cap\partial\Omega} \sum_{l=1}^{L} \Theta_{el} \leq 1/\delta, \tag{2.11}$$

then

$$\overline{w}_K \in I(\overline{u}_K; \overline{u}_{K_e}, e\in\partial K\setminus\partial\Omega; \gamma_{el}, e\in\partial K\cap\partial\Omega, l = 1, \cdots, L), \tag{2.12}$$

where $I(a_1, \ldots, a_n) = [\min\{a_1, \ldots, a_n\}, \max\{a_1, \ldots, a_n\}]$. This is the local maximum principle we were looking for. Let us summarize this result as follows:

Proposition 2.4. *Assume that all the weights of the quadrature rule* (2.3a), ω_l, *are nonnegative. Set* $w_h = u_h + \delta\cdot\Delta t^m \cdot L_h(u_h, \gamma_h)$, *where* u_h *satisfies conditions*

(2.9). *Then, the maximum principle* (2.12) *holds for the elements* $K \in \mathcal{T}_h$ *for which the condition* (2.11)–(2.10) *is satisfied.*

2.4. The $\Lambda\Pi_h$ projection. We now prove that conditions (2.9) can actually be satisfied without compromising the order of accuracy of the method, provided a class of (very general) triangulations is used (the so-called **B**-triangulations), and give a sensible rule for computing the coefficients $\theta_{K,eld}$ and $\eta_{K_e,eld}$. Then, we define a class of local projections $\Lambda\Pi_h$ which enforce conditions (2.9) under a suitable cfl-condition which results from condition (2.11)–(2.10).

Pick an element of the triangulation $\mathcal{T}_h$, say K. We associate with it the vectors

$$\mathbf{d}_{K,e} = \begin{cases} \mathbf{B}_e - \mathbf{B} & \text{if } e \notin \partial\Omega, \\ \mathbf{M}_e - \mathbf{B} & \text{if } e \in \partial\Omega, \end{cases} \tag{2.13a}$$

where $\mathbf{B}$ denotes the barycenter of K, $\mathbf{B}_e$ denotes the one of K_e, and $\mathbf{M}_e$ denotes the midpoint of the edge e. To each point x_{el} of the quadrature rule (2.3a) we associate the vectors

$$\mathbf{d}_{K,el} = x_{el} - \mathbf{B}, \qquad \mathbf{d}_{K_e,el} = x_{el} - \mathbf{B}_e, \tag{2.13b}$$

and express them as linear combinations of the vectors $\mathbf{d}_{K,e}$ as follows:

$$-\mathbf{d}_{K,el} = \theta_{K,ele_1}\mathbf{d}_{K,e_1} + \theta_{K,ele_2}\mathbf{d}_{K,e_2}, \tag{2.13c}$$

$$\mathbf{d}_{K_e,el} = \eta_{K_e,ele_1'}\mathbf{d}_{K,e_1'} + \eta_{K_e,ele_2'}\mathbf{d}_{K,e_2'}. \tag{2.13d}$$

In the figure below we show this construction in the case in which the element K is an interior triangle and the quadrature rule on the edges is the two-point Gauss rule. The quadrature points are indicated by a '$\diamond$'.

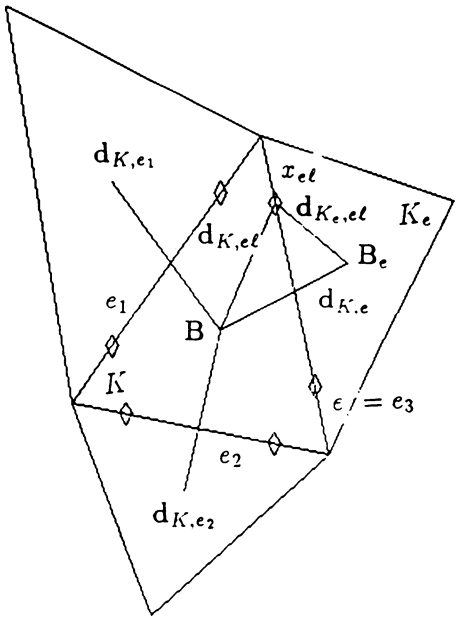

Now, if we associate with $\mathbf{d}_{K,e}$ the value

$$\Delta_{K,e} = \begin{cases} \overline{u}_{K_e} - \overline{u}_K & \text{if } e \notin \partial\Omega, \\ \overline{\gamma}_e - \overline{u}_K & \text{if } e \in \partial\Omega, \end{cases} \tag{2.14a}$$

and with $-\mathbf{d}_{K,el}$ and $\mathbf{d}_{K_e,el}$ the values

$$-\tilde{u}_{K,el} = -u_h(x_{el}^{\text{int}(K)}) + \overline{u}_K, \qquad \tilde{u}_{K_e,el} = u_h(x_{el}^{\text{ext}(K)}) - \overline{u}_{K_e}, \tag{2.14b}$$

respectively, we have

$$\begin{aligned} -\tilde{u}_{K,el} &= [\theta_{K,ele_1}\Delta_{K,e_1} + \theta_{K,ele_2}\Delta_{K,e_2}] + O(h^2), \\ \tilde{u}_{K_e,el} &= [\eta_{K_e,ele_1'}\Delta_{K,e_1'} + \eta_{K_e,ele_2'}\Delta_{K,e_2'}] + O(h^2), \end{aligned} \tag{2.14c}$$

in the sense of the truncation error analysis. (Compare with (2.13c).) Thus, the conditions

$$\tilde{u}_{K,el} \in I(0, b\tilde{U}_{K,el}^{\theta}), \qquad \tilde{u}_{K_e,el} \in I(0, b\tilde{U}_{K,el}^{\eta}),$$

where $b \geq 1$ and

$$\begin{aligned} \tilde{U}_{K,el}^{\theta} &= -[\theta_{K,ele_1}\Delta_{K,e_1} + \theta_{K,ele_2}\Delta_{K,e_2}], \\ \tilde{U}_{K,el}^{\eta} &= [\eta_{K_e,ele_1'}\Delta_{K,e_1'} + \eta_{K_e,ele_2'}\Delta_{K,e_2'}], \end{aligned} \tag{2.15a}$$

are naturally satisfied (in the sense of the truncation error analysis) away from critical points. If M is some upper bound of the second derivatives of u, then the conditions

$$\begin{aligned} &\tilde{u}_{K,el} \in [a_1 - Mh^2, a_2 + Mh^2], \\ &\text{where} \\ &[a_1, a_2] = \begin{cases} [I(0, b\tilde{U}_{K,el}^{\theta})] \cap I(0, b\tilde{U}_{K,el}^{\eta}) & \text{if } e \notin \partial\Omega, \\ I(0, b\tilde{U}_{K,el}^{\theta}) & \text{if } e \in \partial\Omega, \end{cases} \end{aligned} \tag{2.15b}$$

are satisfied uniformly. Moreover, these conditions (with $M = 0$) imply conditions (2.9) provided the coefficients $\theta_{K,eld}$ and $\eta_{K_e,eld'}$ are nonnegative. In order to guarantee this last property, it is clear, from (2.13) and (2.14), that we have to restrict ourselves to consider a special class of triangulations $\mathcal{T}_h$ that we introduce next.

Definition 2.5. A triangulation $\mathcal{T}_h$ is said to be a **B**-triangulation if for each $\mathbf{d}_{K,el}$ and $\mathbf{d}_{K_e,el}$ it is possible to pick the vectors $\mathbf{d}_{K,e_1}$, $\mathbf{d}_{K,e_2}$, $\mathbf{d}_{K,e_1'}$, and $\mathbf{d}_{K,e_2'}$ such that the coefficients θ_{K,ele_1}, θ_{K,ele_2}, $\eta_{K_e,ele_1'}$, and $\eta_{K_e,ele_2'}$ are nonnegative.

Definition 2.6. A family of triangulations $\mathcal{F} = \{\mathcal{T}_h\}_{h>0}$ is said to be **B**-uniform if each triangulation $\mathcal{T}_h$ is a **B**-triangulation, and there is a constant μ such that

$$\theta_{K,eld}, \eta_{K_e,eld'} \in [0, \mu], \quad \forall K \in \mathcal{T}_h, \quad \forall \mathcal{T}_h \in \mathcal{F}. \tag{2.16}$$

In the next subsection we shall give examples of this kind of triangulations. We are now ready to define the $\Lambda\Pi_h$-projections. Let us denote by $\#e(K)$ the number of edges of the element K. The conditions (2.15a) and (2.15b) represent $\#e(K) \times L$ restrictions which, together with the condition

$$\int_K \tilde{u}_h = 0, \tag{2.15c}$$

define a nonempty convex set $C(K; \bar{u}_h) \subset V(K)$. We can now define the projection $\Lambda\Pi_h$ as follows:

$$\begin{aligned} \Lambda\Pi_h : V_h &\longmapsto V_h, \\ u_h &\longmapsto w_h, \end{aligned} \tag{2.17a}$$

such that

$$w_h|_K \text{ is a projection of } u_h|_K \text{ into } C(K; \bar{u}_h). \tag{2.17b}$$

Notice that we did not specify the exact form of the local projection in (2.17b). We can take, for example, the L^2 projection into $C(K; \bar{u}_h)$. In this case, carrying out the projection amounts to solving a minimization problem, which can be reduced to a one-dimensional maximization problem via a duality argument; see [3]. In fact, thanks to (2.14c), in most elements we have $u_h|_K \in C(K; \bar{u}_h)$, and so the operator $\Lambda\Pi_h|_K$ becomes the identity. Thus, if the exact solution is piecewise smooth, it is reasonable, from the computational point of view, to have a 'very complicated' projection into $C(K; \bar{u}_h)$. On the other hand, as the projection is actually carried out only very near the discontinuities, it is not necessary to define it in a very sophisticated way. Some practical implementations of this projection are considered in §3.

Note also that if K is a triangle and $V(K) = P^1(K)$, or $V(K) = P^2(K)$, then from the fact that $w_h \in C(K; \bar{u}_h)$ we deduce easily that there is a constant c_0 such that

$$\|\tilde{w}_h\|_{L^1(K)} \leq c_0 \left\{ \sum_{e \in \partial K} |\bar{u}_K - \bar{u}_{K_e}||e| \right\} h_K, \tag{2.18a}$$

where the constant c_0 depends solely on the parameter σ of the triangulation, see (2.6). The same property is verified if K is a rectangle and $V(K) = Q^1(K)$. We can define $\Lambda\Pi_h|_K$ in order to enforce (2.18a) without damaging the accuracy of the method. If we set

$$\begin{aligned} Z(K, \bar{u}_h) = \{ v_h \in V_h : \text{ if } v_h(x_{el}) = \bar{u}_K, \quad \forall e \in \partial K, \ l = 1, \ldots, L \\ \text{then } v_h(x) = \bar{u}_K, \quad \forall x \in K \}, \end{aligned} \tag{2.17c}$$

and we replace (2.17b) by

$$w_h|_K \text{ is a projection of } u_h|_K \text{ into } C(K; \bar{u}_h) \cap Z(K; \bar{u}_h), \tag{2.17b'}$$

then property (2.18a) is always satisfied.

Thus, we have proven the following result.

Proposition 2.7. *Let* $\Lambda\Pi_h$ *be the projection defined by* (2.17), *with* (2.17b′) *replacing* (2.17b), *and let* $\mathcal{F}$ *be a* **B***-uniform family of triangulations. Set* $w_h = u_h + \delta \cdot \Delta t^m L_h(u_h, \gamma_h)$, *assume that* $u_h = \Lambda\Pi_h(u_h)$, *and suppose that*

$$\overline{u}_h, \gamma_h \in [a, b].$$

Then

$$\overline{w}_h \in [a - Mh^2, b + Mh^2],$$

provided

$$cfl \leq \frac{1}{\delta(1 + 4b\mu)\max\{\#e(K)\}}. \tag{2.19}$$

Moreover,

$$\|\tilde{w}_h\|_{L^1(\Omega)} \leq c_0 \|\overline{w}_h\|_{BV(\Omega)} h, \tag{2.18b}$$

Proof. Property (2.18b) is a simple consequence of (2.18a) and of the definition of the total variation of $\overline{u}_h$:

$$\|\overline{u}_h\|_{BV(\Omega)} = \sum_{K \in \mathcal{T}_h} \left\{ \sum_{e \in \partial K \setminus \partial\Omega} |\overline{u}_K - \overline{u}_{K_e}||e| + \sum_{e \in \partial K \cap \partial\Omega} |\overline{u}_h - \overline{\gamma}_h| \right\},$$

see [12], where we are assuming that $\overline{u}_h(x) = \overline{\gamma}_h(x), \quad \forall x \in \partial\Omega$.

Now, we only have to prove condition (2.19). This condition is nothing but another version of condition (2.11)-(2.10). Consider the following expression:

$$\Psi = \sum_{e \in \partial K \setminus \partial\Omega} \Theta_e + \sum_{e \in \partial K \cap \partial\Omega} \sum_{l=1}^{L} \Theta_{el}.$$

By the definition of Θ_e and Θ_{el}, (2.10), we can write

$$\begin{aligned}
\Psi = & \sum_{e \in \partial K \setminus \partial\Omega} \sum_{l=1}^{L} \frac{\omega_l |e|}{|K|} [-h_{el,2}] \\
& + \sum_{e \in \partial K \setminus \partial\Omega} \sum_{d \in \partial K} \sum_{l=1}^{L} \frac{\omega_l |d|}{|K|} [h_{dl,1}] \theta_{K,dle} \\
& + \sum_{e \in \partial K \setminus \partial\Omega} \sum_{d \in \partial K \setminus \partial\Omega} \sum_{l=1}^{L} \frac{\omega_l |d|}{|K|} [-h_{dl,2}] \eta_{K_d,dle} \\
& + \sum_{e \in \partial K \cap \partial\Omega} \sum_{l=1}^{L} \frac{\omega_l |e|}{|K|} [-h_{el,2}] \\
& + \sum_{e \in \partial K \cap \partial\Omega} \sum_{l=1}^{L} \omega_l \sum_{d \in \partial K} \sum_{l=1}^{L} \frac{\omega_l |d|}{|K|} [h_{dl,1}] \theta_{K,dle} \\
& + \sum_{e \in \partial K \cap \partial\Omega} \sum_{l=1}^{L} \omega_l \sum_{d \in \partial K \setminus \partial\Omega} \sum_{l=1}^{L} \frac{\omega_l |d|}{|K|} [-h_{dl,2}] \eta_{K_d,dle}.
\end{aligned}$$

Thus,

$$\begin{aligned}\Delta t^m \Psi &\le cfl \sum_{e\in\partial K\setminus\partial\Omega} 1 + cfl \sum_{e\in\partial K}\sum_{d\in\partial K}\sum_{l=1}^{L}\omega_l\theta_{K,dle} \\ &\quad + cfl \sum_{e\in\partial K}\sum_{d\in\partial K\setminus\partial\Omega}\sum_{l=1}^{L}\omega_l\eta_{K_d,dle} \\ &\le cfl\left[\#e(K) + \sum_{d\in\partial K}\sum_{l=1}^{L}\omega_l\sum_{e\in\partial K}\theta_{K,dle}\right. \\ &\qquad\left. + \sum_{d\in\partial K\setminus\partial\Omega}\sum_{l=1}^{L}\omega_l\sum_{e\in\partial K}\eta_{K_d,dle}\right] \\ &\le cfl\left[\#e(K) + \sum_{d\in\partial K}\sum_{l=1}^{L}\omega_l\, 4b\mu\right] \le cfl\,\#e(K)[1+4b\mu].\end{aligned}$$

This proves the result. □

In this way, we have obtained a class of local projections $\Lambda\Pi_h$ which enforce maximum principles on the RKDG methods. In particular, if we set $M = 0$, Proposition 2.7 and Lemma 2.3 guarantee that $u_h \in [a_0, b_0]$ provided $u_0, \gamma_h \in [a_0, b_0]$. Notice, however, that there are some values of the boundary data γ_h which are irrelevant and should not be taken into consideration when carrying out the projection $\Lambda\Pi_h$, for they could destroy the accuracy of the methods. Those values are the so-called outflow values, i.e., the values γ_{el} such that $\mathbf{f}'(\gamma_{el})\cdot\mathbf{n}_{e,K} > 0$. Thus, to avoid this inconvenience, we simply replace γ_{el} by

$$\gamma'_{el} = \begin{cases} \gamma_{el} & \text{if } \mathbf{f}'(\gamma_{el})\cdot\mathbf{n}_{e,K} \le 0, \\ \tilde{U}^{\theta}_{el} & \text{otherwise,}\end{cases} \tag{2.20}$$

in (2.9). This completes our treatment of boundary conditions. Proposition 2.7 remains valid in this case.

2.5. On B-triangulations. We now give two main examples of **B**-uniform families of triangulations. We begin with a very simple result, which shows that a **B**-uniform family of triangulations need not be regular.

Proposition 2.8. *Let $\mathcal{F}$ be a family of triangulations made of rectangles. Then $\mathcal{F}$ is a* **B***-uniform family. Moreover, $\mu = 1$ in* (2.16).

A more delicate case is the following.

Proposition 2.9. *Let $\mathcal{F}$ be a regular family of triangulations made of acute triangles. Then $\mathcal{F}$ is a* **B***-uniform family. Moreover, $\mu = 2\sigma^3(1+\sigma^2)^{3/2}$, where σ is the constant in* (2.6).

Proof. First, let us prove that each triangulation $\mathcal{T}_h \in \mathcal{F}$ is a **B**-triangulation. Consider the figure below. The straight line l is parallel to $\mathbf{a}_2 - \mathbf{a}_1$, the line l_1 is parallel to $\mathbf{b}_1 - \mathbf{a}_2$, and the line l_2 to $\mathbf{b}_2 - \mathbf{a}_1$. The point $\mathbf{P}_i$ is the intersection of l with l_i, $i = 1, 2$. The triangle whose barycenter is $\mathbf{B}$ (resp., $\mathbf{B}_i$) will be denoted by T (resp., T_i). We shall prove that the angle $(\alpha_1 + \alpha_2)$ is bounded below by a positive constant depending solely on σ. This implies that $\mathcal{T}_h$ is a **B**-triangulation.

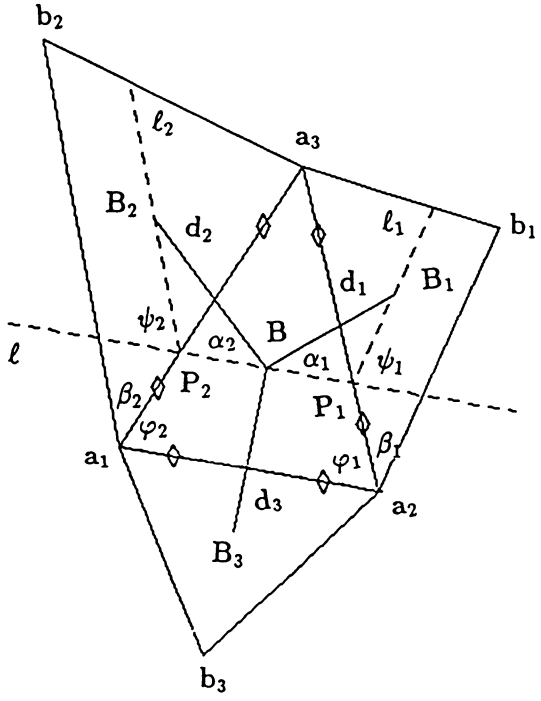

Note that

$$|\mathbf{B}_1 - \mathbf{B}| \sin \alpha_1 = |\mathbf{B}_1 - \mathbf{P}_1| \sin \psi_1.$$

By construction, $\mathbf{B}_1 - \mathbf{B} = \frac{1}{3}(\mathbf{b}_1 - \mathbf{a}_1) = \frac{1}{3}(\mathbf{b}_1 - \mathbf{a}_2) + \frac{1}{3}(\mathbf{a}_2 - \mathbf{a}_1)$, and $\mathbf{B}_1 - \mathbf{P}_1 = \frac{1}{3}(\mathbf{b}_1 - \mathbf{a}_2)$. Thus

$$\sin \alpha_1 \geq \frac{|\mathbf{b}_1 - \mathbf{a}_2|}{|\mathbf{b}_1 - \mathbf{a}_2| + |\mathbf{a}_2 - \mathbf{a}_1|} \sin \psi_1.$$

By the regularity condition (2.6) we have:

$$\frac{1}{\sigma} \leq \frac{|\mathbf{a}_2 - \mathbf{a}_1|}{|\mathbf{a}_2 - \mathbf{a}_3|} \leq \sigma, \qquad \frac{1}{\sigma} \leq \frac{|\mathbf{a}_2 - \mathbf{a}_3|}{|\mathbf{b}_1 - \mathbf{a}_2|} \leq \sigma,$$

and so

$$\sin\alpha_1 \geq \frac{1}{1+\sigma^2}\sin\psi_1.$$

If we set $\cot\alpha_0 = \sigma$, the regularity condition (2.6) can be restated as follows: every angle of K is larger than $2\alpha_0$. This is the so-called Zlámal condition, see [4, Exercise 3.1.3]. Thus,

$$\psi_1 = \pi - \varphi_1 - \beta_1 \in \left[\frac{\pi}{2} - \varphi_1,\ \pi - 2\alpha_0 - \varphi_1\right],$$
$$\psi_2 = \pi - \varphi_2 - \beta_2 \in \left[\frac{\pi}{2} - \varphi_2,\ \pi - 2\alpha_0 - \varphi_2\right].$$

If $\psi_1 \geq \frac{\pi}{2}$, then $\sin\psi_1 \geq \sin 4\alpha_0$. If $\psi_1 \in [\frac{\pi}{2} - \varphi_1, \frac{\pi}{2}]$, then $\sin\psi_1 \geq \sin(\frac{\pi}{2} - \varphi_1)$. If ψ_1 and ψ_2 are smaller than $\frac{\pi}{2}$, then

$$\begin{aligned}\max\{\sin\psi_1,\ \sin\psi_2\} &\geq \max\left\{\sin\left(\frac{\pi}{2} - \varphi_1\right),\ \sin\left(\frac{\pi}{2} - \varphi_2\right)\right\}\\ &\geq \inf_{\varphi_1,\varphi_2} \max\left\{\sin\left(\frac{\pi}{2} - \varphi_1\right),\ \sin\left(\frac{\pi}{2} - \varphi_2\right)\right\}.\end{aligned}$$

By symmetry, the infimum is attained when $\varphi_1 = \varphi_2 = \varphi$, so that $\frac{\pi}{2} - \varphi = \frac{\varphi_3}{2} \geq \alpha_0$, and so $\max\{\sin\psi_1, \sin\psi_2\} \geq \sin\alpha_0$.

As a consequence,

$$\max\{\sin\alpha_1, \sin\alpha_2\} \geq \sin^3\alpha_0 = (1+\sigma^2)^{-3/2},$$

which implies that $(\alpha_1 + \alpha_2)$ is uniformly bounded from below by a strictly positive constant depending solely on σ. This shows that any vector can be written either as a negative combination of the vectors $\mathbf{d}_1$, $\mathbf{d}_2$, and $\mathbf{d}_3$, or as a positive combination of them. This implies that $\mathscr{F}$ is a family of **B**-triangulations.

Now let us prove the estimate for μ. Set $\mathbf{d} = \nu_1\mathbf{d}_1 + \nu_2\mathbf{d}_2$, where the coefficients ν_i are nonnegative. Let ξ_{12} be the angle between $\mathbf{d}_1$ and $\mathbf{d}_2$, and let ξ be the one between $\mathbf{d}$ and $\mathbf{d}_2$. Let us estimate ν_1. By definition,

$$\nu_1 = -\frac{\mathbf{d}\cdot\mathbf{d}_2^{\perp}}{\mathbf{d}_1\cdot\mathbf{d}_2^{\perp}} \leq \frac{|\mathbf{d}|}{|\mathbf{d}_1|}\cdot\frac{|\sin\xi|}{|\sin\xi_{12}|}.$$

If $\xi_{12} \in [0, \pi/2]$, then $\xi \in [0, \xi_{12}]$, and so $\frac{|\sin\xi|}{|\sin\xi_{12}|} \leq 1$. If $\xi_{12} \in [\pi/2, \pi]$, then $\alpha_1 + \alpha_2 = \pi - \xi_{12} \in [0, \pi/2)$, and so

$$\sin\xi_{12} \geq \max\{\sin\alpha_1,\ \sin\alpha_2\} \geq \sin^3\alpha_0.$$

Thus,

$$\nu_1 \leq \frac{|\mathbf{d}|}{|\mathbf{d}_1|} \cdot \sin^{-3} \alpha_0.$$

But, by construction, $|\mathbf{d}_1| = \frac{1}{3}|\mathbf{b}_1 - \mathbf{a}_1|$. If the edge $\mathbf{a}_2\,\mathbf{a}_3$ lies on $\partial\Omega$, then $\mathbf{b}_1$ is the midpoint of it, by construction. This implies that $|\mathbf{d}_1| \geq \rho_T/3$. If the edge $\mathbf{a}_2\,\mathbf{a}_3$ does not lie on $\partial\Omega$, a simple calculation shows that $|\mathbf{d}_1| \geq (1 + \frac{1}{\sigma^2})\rho_T/3$. The regularity of the triangulation has strongly been used in this last step. Thus, we always have that $|\mathbf{d}_1| \geq \rho_T/3$.

It remains to estimate $|\mathbf{d}|$. The cases of interest are when (i) $\mathbf{B} + \mathbf{d}$ lies on the border of the triangle T, and when (ii) $\mathbf{B}_i + \mathbf{d}$ lies on the border of the triangle T, for $i = 1, 2, 3$. The first case corresponds to the equation (2.13c), whereas the second corresponds to equation (2.13d). In the first case we simply have $|\mathbf{d}| \leq 2h_T/3$. In the second we obtain $|\mathbf{d}| \leq 2h_{T_i}/3 \leq 2\sigma^2 h_T/3$, as a consequence of the regularity of the triangulation. As $\sigma \geq \sqrt{3}$, we have $|\mathbf{d}| \leq 2\sigma^2 h_T/3$ in all the cases under consideration. Thus,

$$\nu_1 \leq \frac{2\sigma^2 h_T/3}{\rho_T/3} \sin^{-3}(\alpha_0) \leq 2\sigma^3(1+\sigma^2)^{3/2}.$$

This proves the result. □

2.6. Stability and convergence. We summarize the results obtained above in the following theorem.

Theorem 2.10. *Consider the RKDG method* (2.1), *where the operator* L_h *is defined by* (2.5)–(2.4)–(2.3)–(2.2), *and the projection* $\Lambda\Pi_h$ *is defined by* (2.17)–(2.15)–(2.20). *Assume that the family of triangulations* $\mathcal{F}$ *is regular and* **B***-uniform. Suppose that* $V(K) \supset P^k(K)$, $\forall K \in \mathcal{T}_h$, $\forall \mathcal{T}_h \in \mathcal{F}$, *and that the quadrature rule over the edges is exact for polynomials of degree* $(2k+1)$, *and the quadrature rule over the elements is exact for polynomials of degree* $2k$. *Then:*

(1) *The RKDG method is formally uniformly* $(k+1)$*st-order accurate in time and space if* $\Delta t = O(h)$;

(2) *the approximate solution generated by the RKDG method verifies the maximum principle* (2.8) *if the cfl-condition* (2.19) *is verified with* $\delta = \max_{i,l} |\frac{\beta_{i,l}}{\alpha_{i,l}}|$;

(3) *the approximate solution converges to a weak solution of* (1.1) *if there is a constant* C *such that* $\|\overline{u}_h\|_{BV(\Omega)} \leq C$.

The proof of (3) is similar to the proof of the same result for the one-dimensional case and will be omitted; see [7].

3. Numerical results

In this section we display some preliminary numerical results. Extensive computations, in which we explore numerically several fluxes, triangulations,

finite elements, quadrature rules, and local projections, are the subject of a forthcoming paper.

We consider triangulations made only of triangles (see Figure 1), and we take the local finite element space $V(T)$ to be $P^1(T)$, i.e., the space of linear functions on T. Proposition 2.1 affirms that we can reach a second-order accurate space approximation (which is in fact the best possible order of accuracy that can be reached with the given elements), provided we take a quadrature rule for the edges exact for polynomials of degree 3, and a quadrature rule for the elements exact for polynomials of P^2. Accordingly, we take the two-point Gauss quadrature rule for the edges, and the three midpoint rule for the triangles. We take the Godunov flux as the flux $h_{e,T}$, and the Runge-Kutta time discretization parameters of order two; see Table 1. To complete the definition of this RKDG^1 method (which is formally uniformly second-order accurate) we need to specify the local projection, $\Lambda\Pi_h$.

This projection is defined as described in subsection 2.4, only, the points x_{el} associated with the quadrature rule of the edges are replaced by the points associated with the degrees of freedom, the midpoints of the edges. In this way, four conditions are to be enforced by the projection on each triangle. Each of the degrees of freedom generates a single condition (2.15b). The fourth is provided by the conservativity condition (2.15c). First, the projection $\Lambda\Pi_h$ enforces each of the conditions (2.15b) independently of each other. This constitutes three simple one-dimensional projections. After this step, the conservativity condition (2.15c) is enforced via a trivial arithmetic computation which leaves the conditions (2.15b) satisfied.

It is important to stress the fact that the choice of the degrees of freedom as the values at the midpoints of the edges of each triangle increases the computational efficiency of the method. It allows us to save time in the evaluation of the integral over the triangles, and it allows us to define a simple and efficient local projection $\Lambda\Pi_h$.

We are going to test the RKDG^1 method described above in three examples. We point out that we compute the L^∞ error on the triangle T by evaluating the error at the barycenter. The $L^1(T)$ error is obtained by multiplying that value by the area of the triangle. The errors are evaluated over the whole domain, unless otherwise stated. The L^1 error is divided by the area of the domain over which it has been computed. We also need to comment about the graphic outputs. A given function v, which is typically either the exact solution, or its finite element approximation, is represented graphically as a surface (and its level curves). To obtain such a surface, we evaluate the function u at each of the points of a 70×70 uniform grid. Then, we interpolate them linearly. Finally, in the figures in which we display cuts along the diagonal of the domain Ω, the solid line always represents the exact solution. The '+' represent the approximate solution. A single '+' per triangle has been displayed.

Example 1. In this problem, we test the capability of the method to achieve

uniform second-order accuracy away from discontinuities. We consider the two-dimensional version of Burgers' equation with periodic boundary conditions:

$$
\begin{aligned}
&\partial_t u + \partial_x(u^2/2) + \partial_y(u^2/2) = 0 && \text{in } (0, T) \times \Omega, \\
&u(t = 0, x, y) = \frac{1}{4} + \frac{1}{2}\sin(\pi(x + y)), && (x, y) \in \Omega,
\end{aligned} \tag{3.1}
$$

where the domain Ω is the square $[-1, 1] \times [-1, 1]$. We take $M = 20$, and $b = 3$ in (2.15b). The triangulations $\mathcal{T}_{h,\text{unif}}$ are like the one displayed on Figure 1 (top). (Notice that in that figure $h = 1/16$.)

At $T = 0.1$ the exact solution is smooth, see Figure 2. In Table 2, the L^1 and L^∞ errors at $T = 0.1$ are displayed. The approximate solution (associated with the triangulation of Figure 1 (top)) is shown in Figure 3 and Figure 6 (top). Uniform second-order accuracy has been achieved.

At $T = 0.45$, the exact solution presents a discontinuity curve, see Figure 4. The errors away from the discontinuity curve are shown in Table 3. The approximate solution is displayed in Figure 5 and Figure 6 (bottom). Again, uniform second-order accuracy has been achieved away from discontinuities. Notice how the discontinuity curve has been captured within a single element, see Figure 6 (bottom).

Example 2. In this problem, we test the boundary treatment of the method. We consider the preceding equations, but this time we impose a boundary condition:

$$
\begin{aligned}
&\partial_t u + \partial_x(u^2/2) + \partial_y(u^2/2) = 0 && \text{in } (0, T) \times \Omega, \\
&u(t = 0, x, y) = \frac{1}{4} + \frac{1}{2}\sin(\pi(x + y)), && (x, y) \in \Omega, \\
&u(t, x, y) = v(t, x, y), && (x, y) \in \partial\Omega,
\end{aligned} \tag{3.2}
$$

where v is the exact solution of problem (3.1). See [1] for a suitable interpretation of the boundary conditions. The exact solution of this problem coincides with the one of problem (3.1). Notice that since we use a pure upwind monotone flux, the outflow boundary condition, even if provided redundantly, is never used in the computation. All the discretization parameters are the same as in the preceding example.

The results are indistiguishable from the ones of the preceding problem. The L^∞ errors are the same as those displayed in Tables 2 and 3. Thus, the boundary treatment does not introduce any spurious oscillation, maintains the maximum principle, and does not destroy the uniform accuracy of the method.

Example 3. In this last example we test the convergence of the method in the case of nonconvex fluxes. We also test the ability of the method to take advantage of nonuniform triangulations. Consider the initial-boundary value

problem:

$$\partial_t u + \partial_x f(u) + \partial_y f(u) = 0 \quad \text{in } (0, T) \times \Omega,$$

$$u(t=0, x, y) = \begin{cases} 7/8 & \text{for } x > 0 \text{ and } y > 0, \\ 0 & \text{for } x < 0 \text{ and } y > 0, \\ 1/4 & \text{for } x < 0 \text{ and } y < 0, \\ 0 & \text{for } x > 0 \text{ and } y < 0, \end{cases} \qquad (x, y) \in \Omega, \tag{3.3}$$

$$u(t, x, y) = v(t, x, y), \qquad (x, y) \in \partial\Omega,$$

where $f(u) = 5(1/8 + (u - 1/2)^3)$, Ω is the square $[-1, 1] \times [-1, 1]$, and v is the exact solution of the corresponding Riemann problem. The exact solution has been computed following [29], and is displayed in Figure 7 for $T = 1$. We take $M = 0$ and $b = 3$. In Table 4, we can see that convergence to the entropy solution is achieved.

In Figures 8, 9, and 10 we display the approximate solutions. The approximate solution of Figure 8 is defined on a triangulation whose triangles do not match the discontinuity curve. Nevertheless, the curve has been captured within two triangles, except at its cusp. The approximate solution of Figure 9 has, on the contrary, been defined on a triangulation designed to fit the discontinuity curve, and to better resolve the structure of the cusp. An excellent capture of discontinuities can be observed. See also Figure 10. In Table 5 we compare the L^1 errors of the approximate solutions under consideration.

In conclusion, the numerical results show that (i) the RKDG^1 method is uniformly second-order accurate away from discontinuities, that (ii) it does take advantage of suitable (nonuniform) triangulations, that (iii) it can resolve very complicated structures of the discontinuity curves, and that (iv) it converges to the entropy solution, even when the fluxes are nonconvex.

4. Concluding remarks

This paper is the fourth of a series, [5, 6, 7], in which we introduce, analyze, and test a new class of methods for numerically solving nonlinear hyperbolic conservation laws. These methods are called Runge-Kutta Discontinuous Galerkin Methods. In the previous papers, the one-dimensional case, $d = 1$, has been considered. In this paper we consider the multidimensional scalar case. A general theory for these schemes has been developed. These methods can easily handle complicated geometries, for they can be defined using quite arbitrary triangulations. For the so-called uniform triangulations, these methods are formally uniformly $(k+1)$st-order accurate (when $\Delta t = O(\Delta x)$). They can easily handle the boundary conditions. They also verify a suitable maximum principle for general nonlinearities, if the triangulations are **B**-triangulations, a concept introduced in this paper. The methods are easy to code, and show high-order uniform accuracy, good capture of discontinuity curves, and convergence to the entropy solution, even for nonconvex nonlinearities. Extensive computational experiments for the scalar case, as well as extensions to two-dimensional systems, constitute the subject of ongoing work.

TABLE 2
Example 1. Initial value problem (3.1), $T = 0.1$.

	L^∞		L^1	
h	$10^4 \cdot$ error	order	$10^4 \cdot$ error	order
1/2	500.92	–	248.55	–
1/4	118.20	2.08	61.27	2.02
1/8	37.27	1.67	15.04	2.03
1/16	8.65	2.11	3.73	2.01
1/32	2.20	1.97	0.94	1.99

TABLE 3
Example 1. Initial value problem (3.1), $T = 0.45$. The errors are computed in the region $[-0.2, 0.4] \times [-0.2, 0.4]$.

	L^∞		L^1	
h	$10^4 \cdot$ error	order	$10^4 \cdot$ error	order
1/2	63.71	–	23.61	–
1/4	8.38	2.93	2.52	3.05
1/8	3.92	1.10	0.72	1.98
1/16	0.92	2.09	0.17	2.10
1/32	0.22	2.07	0.03	2.39

TABLE 4
Example 3. Initial-boundary value problem (3.3), $T = 1$.

	L^1	
h	$10^1 \cdot$ error	order
1/2	7.17	-
1/4	4.73	0.60
1/8	2.92	0.69
1/16	1.71	0.77
1/32	0.99	0.78

TABLE 5
Example 3. Initial-boundary value problem (3.3), $T = 1$.
Effect of the triangulation on the overall L^1 error.

triangulation	number of elements	$10^1 \cdot$ error
$\mathcal{T}_{h=1/16,\,\mathrm{unif}}$	2048	1.71
$\mathcal{T}_{h,\,\mathrm{nonunif}}$	2048	0.89
$\mathcal{T}_{h=1/32,\,\mathrm{unif}}$	8192	0.99

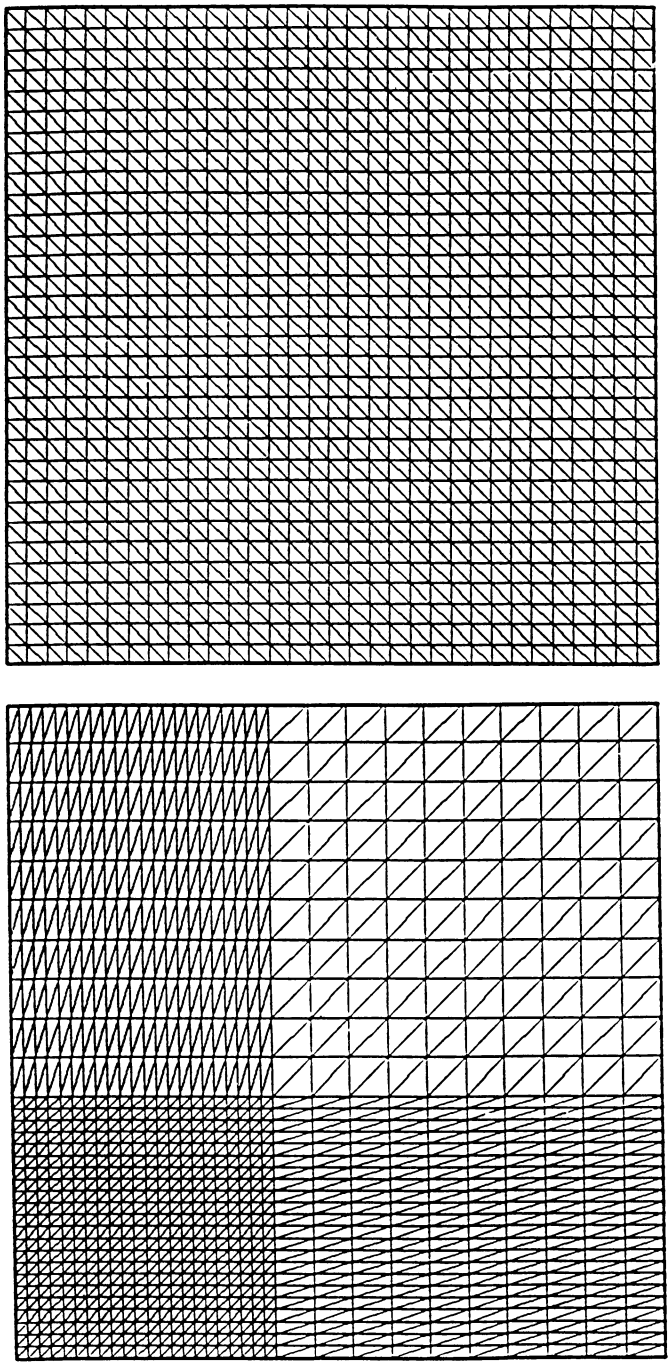

FIGURE 1. The triangulations: $\mathcal{T}_{h=1/16,\,\mathrm{unif}}$ (on top) and $\mathcal{T}_{h,\,\mathrm{nonunif}}$. Both triangulations have $32 \times 32 \times 2 = 2048$ elements.

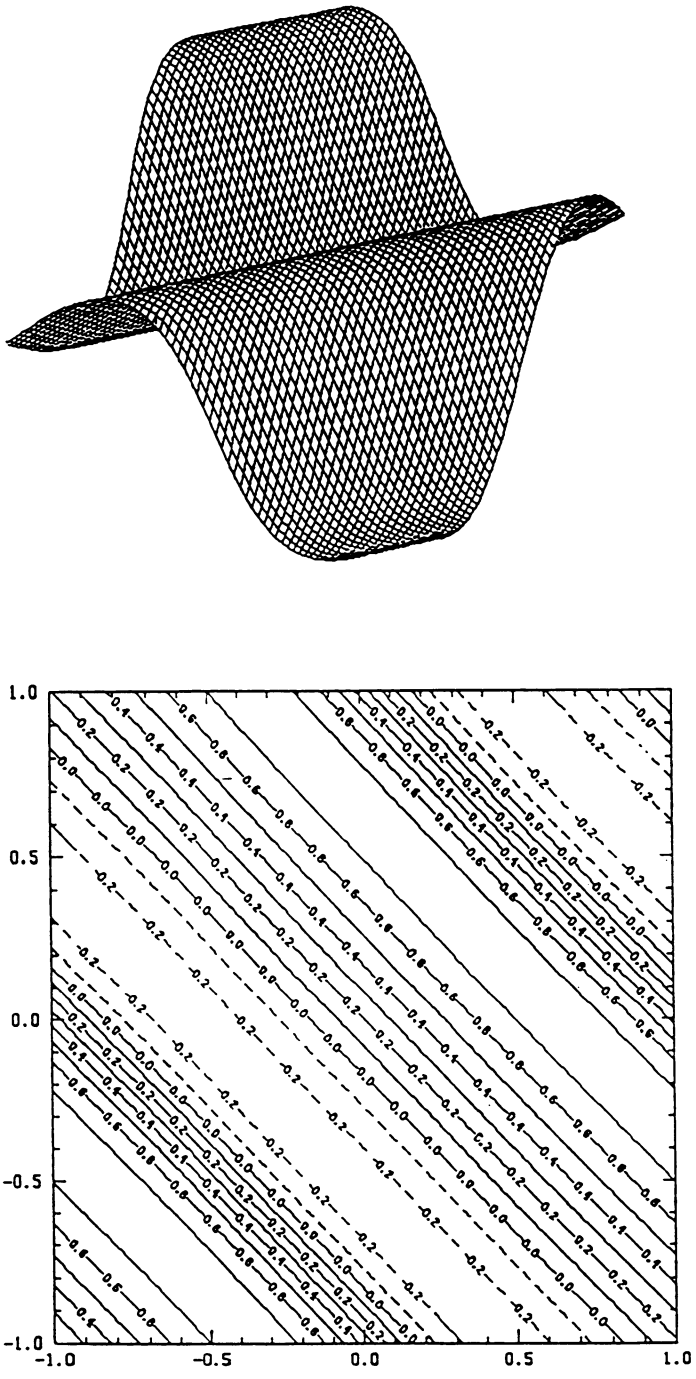

FIGURE 2. The exact solution. Initial value problem (3.1), $T = 0.1$.

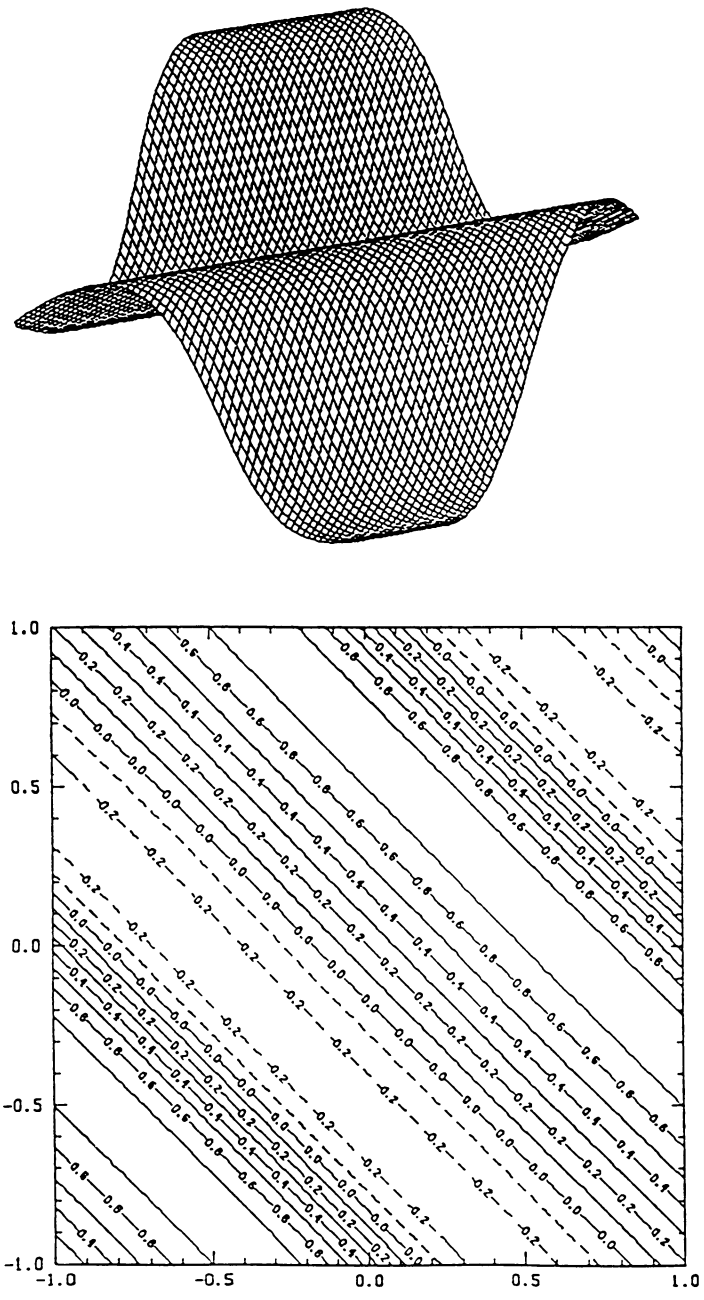

FIGURE 3. The approximate solution. Initial value problem (3.1), $T = 0.1$.
The triangulation is $\mathcal{T}_{h=1/16,\,\mathrm{unif}}$, $cfl = 0.21$.

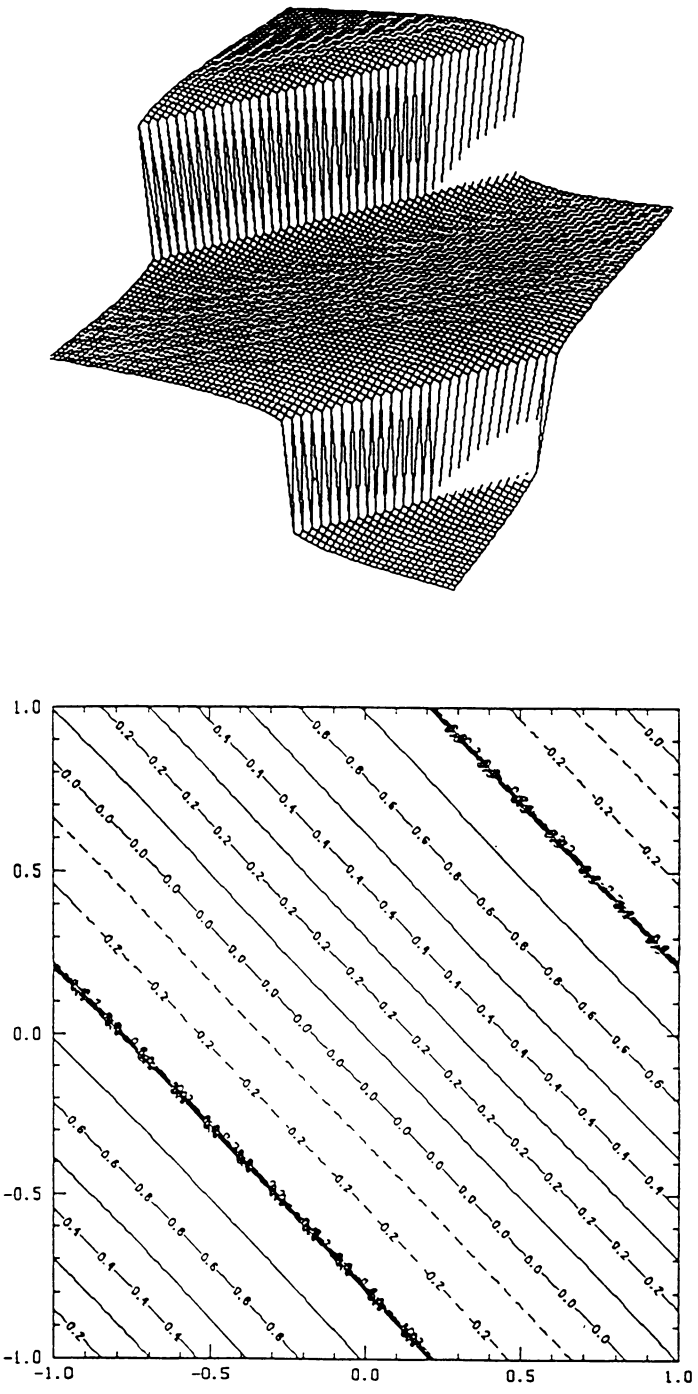

FIGURE 4. The exact solution. Initial value problem (3.1), $T = 0.45$.

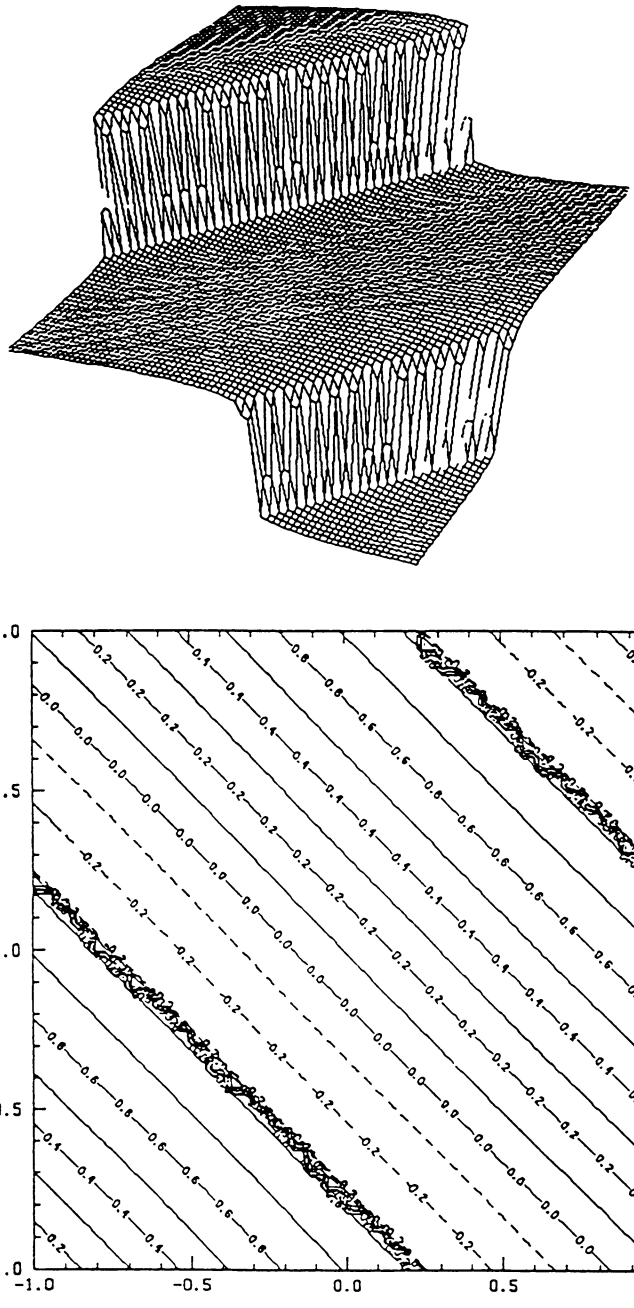

FIGURE 5. The approximate solution. Initial value problem (3.1), $T = 0.45$.
The triangulation is $\mathcal{T}_{h=1/16,\,\mathrm{unif}}$, $cfl = 0.21$.

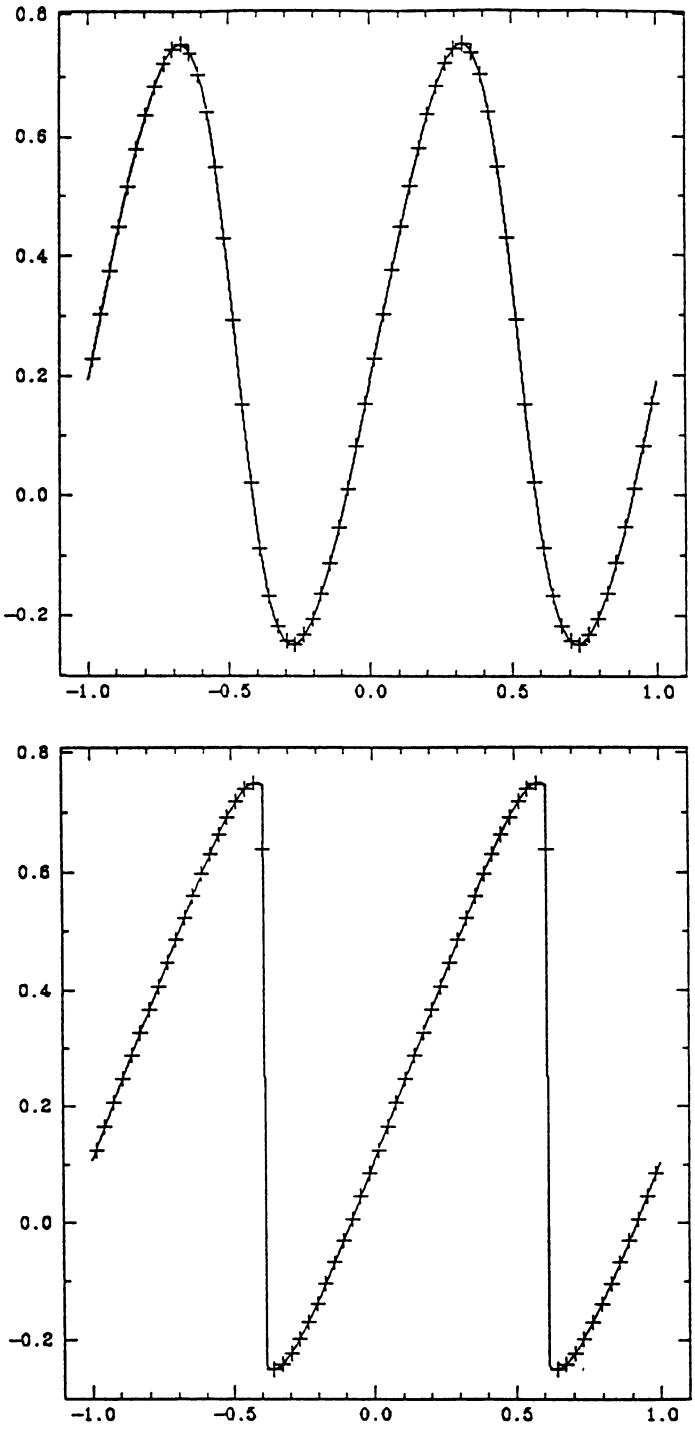

FIGURE 6. Initial value problem (3.1). Cut along the diagonal.
Top: $T = 0.1$, bottom: $T = 0.45$.

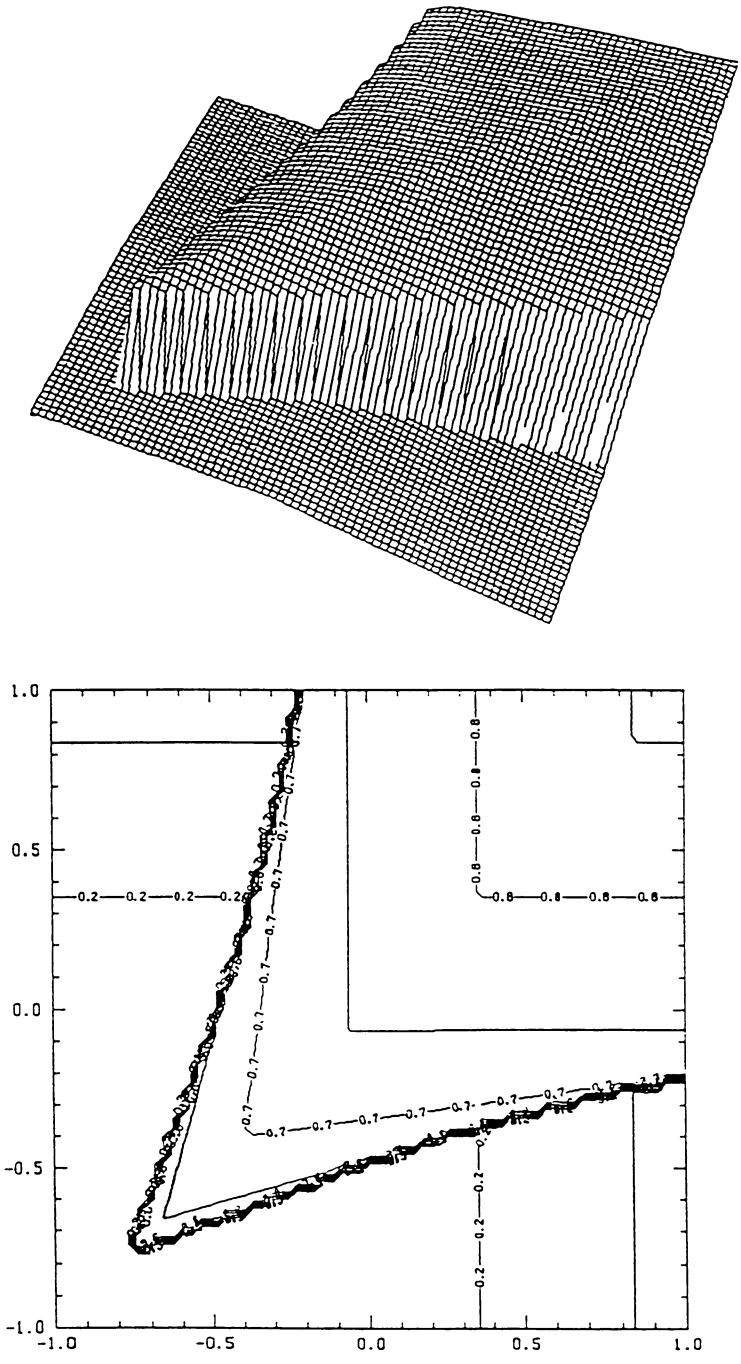

FIGURE 7. The exact solution. Initial value problem (3.3), $T = 1$.

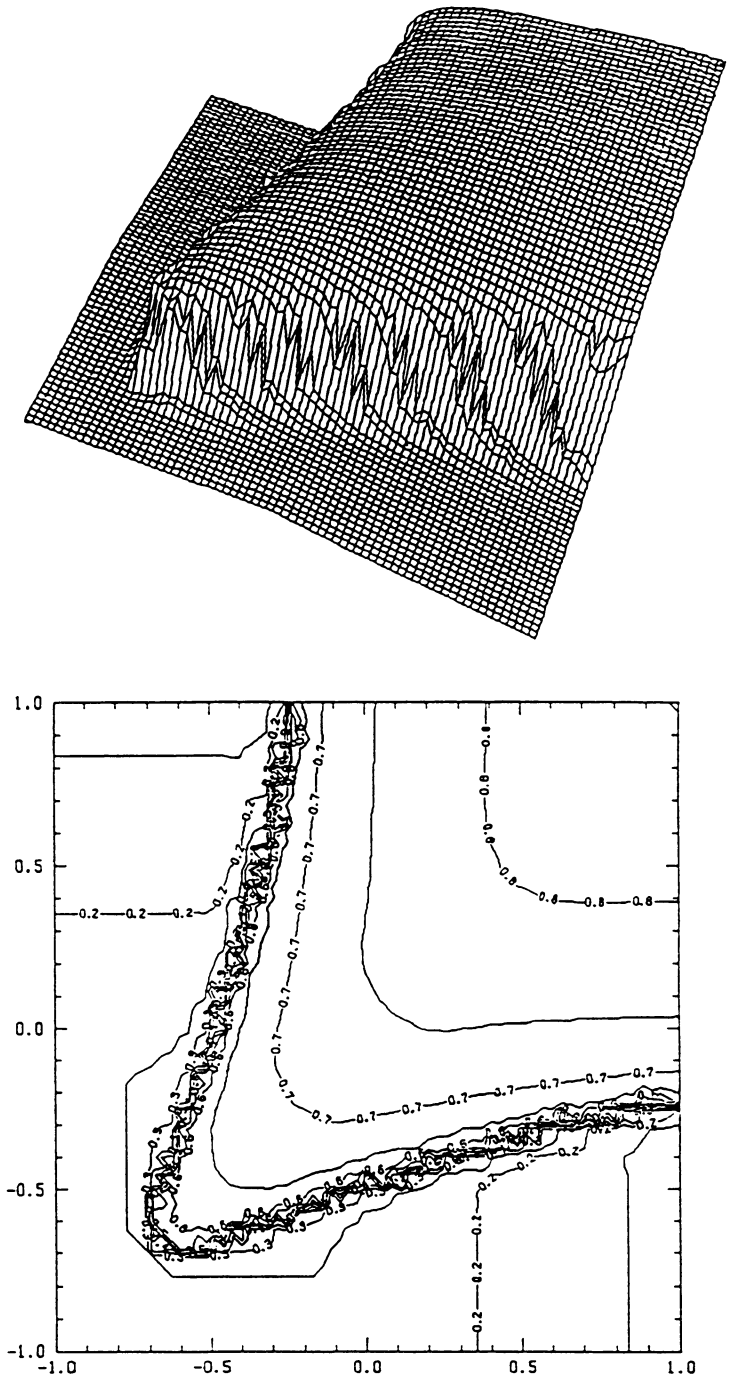

FIGURE 8. The approximate solution. Initial-boundary value problem (3.3), $T = 1$. The triangulation is $\mathcal{T}_{h=1/16,\,\mathrm{unif}}$, $cfl = 0.59$.

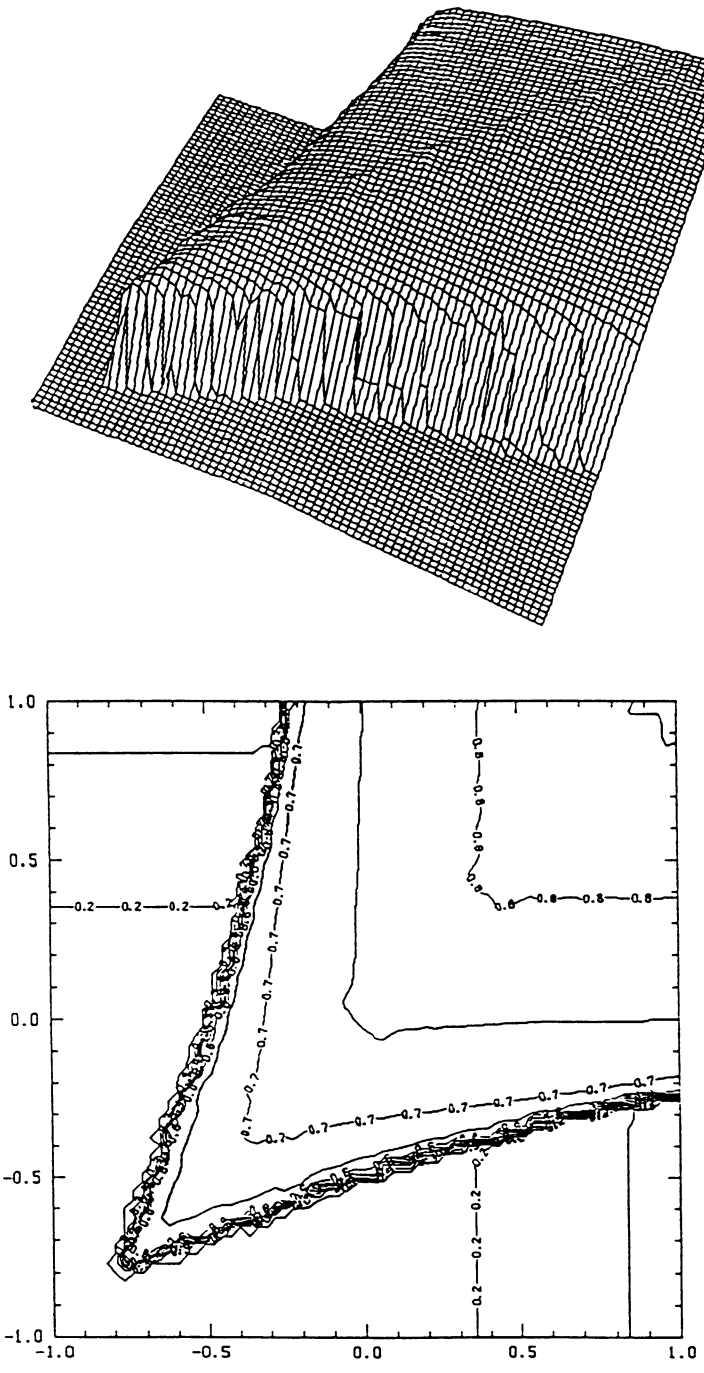

FIGURE 9. The approximate solution. Initial-boundary value problem (3.3), $T = 1$. The triangulation is $\mathcal{T}_{h,\text{nonunif}}$, $cfl = 0.59$.

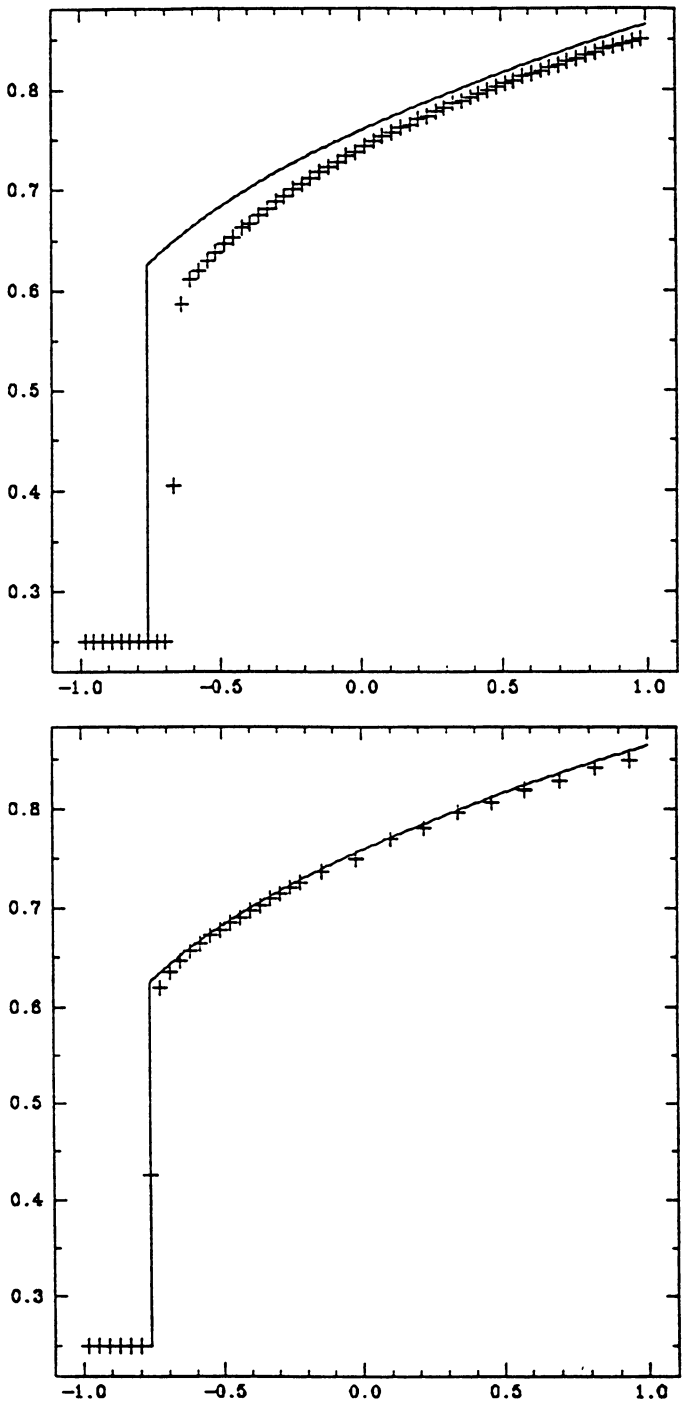

FIGURE 10. Initial-boundary value problem (3.3). Cut along the diagonal. Top: triangulation $\mathcal{T}_{h=1/16,\,\mathrm{unif}}$, bottom: triangulation $\mathcal{T}_{h,\,\mathrm{nonunif}}$.

BIBLIOGRAPHY

1. C. Bardos, A. Y. LeRoux and J. C. Nedelec, *First order quasilinear equations with boundary conditions*, Comm. Partial Differential Equations **4** (1979), 1017–1034.
2. J. B. Bell, C. N. Dawson, and G. R. Shubin, *An unsplit, higher-order Godunov method for scalar conservation laws in multiple dimensions*, J. Comput. Phys. **74** (1988), 1–24.
3. G. Chavent, B. Cockburn, G. Cohen, and J. Jaffré, *A discontinuous finite element method for nonlinear hyperbolic equations*, Innovative Numerical Methods in Engineering (Proc. 4th Internat. Sympos. (Georgia Institute of Technology, Atlanta, Georgia), Springer-Verlag, 1986, pp. 337-342.
4. P. G. Ciarlet, *The finite element method for elliptic problems*, North-Holland, Amsterdam, 1975.
5. B. Cockburn and C.-W. Shu, *The Runge–Kutta local projection P^1 discontinuous Galerkin finite element method for scalar conservation laws*, Institute for Mathematics and its Applications Preprint Series # 388, Univ. of Minnesota (1988); Proceedings of First National Fluid Dynamics Congress, Cincinnati, Ohio, July 24-28, 1988; to appear in M^2AN.
6. ———, *TVB Runge–Kutta local projection discontinuous Galerkin finite element method for conservation laws* II: *General framework*, Math. Comp. **52** (1989), 411–435.
7. B. Cockburn, S.-Y. Lin, and C.-W. Shu, *TVB Runge–Kutta local projection discontinuous-Galerkin finite element method for conservation laws* III: *One-dimensional systems*, J. Comput. Phys. **84** (1989), 90–113.
8. B. Cockburn, *Quasimonotone schemes for scalar conservation laws,* I, SIAM J. Numer. Anal. **26** (1989), 1325–1341.
9. ———, *Quasimonotone schemes for scalar conservation laws,* II, SIAM J. Numer. Anal. **27** (1990), 247–258.
10. ———, *Quasimonotone schemes for scalar conservation laws,* III, SIAM J. Numer. Anal. **27** (1990), 259–276.
11. M. Crandall and A. Majda, *Monotone difference approximations for scalar conservation laws*, Math. Comp. **34** (1980), 1-21.
12. E. Giusti, *Minimal surfaces and functions of bounded variation*, Birkhäuser, Basel, 1984.
13. J. Goodman and R. LeVeque, *On the accuracy of stable schemes for 2D scalar conservation laws*, Math. Comp. **45** (1985), 15–21.
14. A. Harten, *On a class of high-resolution total-variation-stable finite-difference schemes*, SIAM J. Numer. Anal. **21** (1984), 1-23.
15. ———, *Preliminary results on the extension of ENO schemes to two-dimensional problems*, in Proceedings of the International Conference on Hyperbolic Problems, Saint-Etienne, January 1986.
16. ———, *ENO schemes with subcell resolutions*, J. Comput. Phys. **83** (1989), pp. 148–184.
17. A. Harten and S. Osher, *Uniformly high-order accurate nonoscillatory schemes,* I, SIAM J. Numer. Anal. **24** (1987), 279–309.
18. A. Harten, B. Engquist, S. Osher, and S. Chakravarthy, *Uniformly high-order accurate nonoscillatory schemes,* III, J. Comput. Phys. **71** (1987), 231–303.
19. T. Hughes and A. Brook, *Streamline Upwind–Petrov–Galerkin formulations for convection dominated flows with particular emphasis on the incompressible Navier–Stokes equations*, Comput. Methods Appl. Mech. Engrg. **32** (1982), 199–259.
20. T. Hughes and M. Mallet, *A high-precision finite element method for shock-tube calculations*, Finite Elements in Fluids, vol. 6 (R. H. Gallagher, G. F. Carey, J. T. Oden, and O. C. Zienkiewicz, eds.), 1985, pp. 339–353.

21. T. Hughes, L. P. Franca, M. Mallet and A. Misukami, *A new finite element formulation for computational fluid dynamics,* I, Comput. Methods Appl. Mech. Engrg. **54** (1986), 223–234.
22. ——, *A new finite element formulation for computational fluid dynamics,* II, Comput. Methods Appl. Mech. Engrg. **54** (1986), 341–355.
23. ——, *A new finite element formulation for computational fluid dynamics,* III, Comput. Methods Appl. Mech. Engrg. **58** (1986), 305–328.
24. ——, *A new finite element formulation for computational fluid dynamics,* IV, Comput. Methods Appl. Mech. Engrg. **58** (1986), 329–336.
25. C. Johnson and J. Saranen, *Streamline diffusion methods for problems in fluid mechanics*, Math. Comp. **47** (1986), 1–18.
26. C. Johnson and A. Szepessy, *On the convergence of a finite element method for a nonlinear hyperbolic conservation law*, Math. Comp. **49** (1987), 427–444.
27. C. Johnson, A. Szepessy and P. Hansbo, *On the convergence of shock-capturing streamline diffusion finite element methods for hyperbolic conservation laws*, Math. Comp. **54** (1990), 107–129.
28. W. B. Lindquist, *The scalar Riemann problem in two spatial dimensions: piecewise smoothness of solutions and its breakdown*, SIAM J. Math. Anal. **17** (1986), 1178–1197.
29. ——, *Construction of solutions for two-dimensional Riemann problems*, Comput. Math. Appl. **12A** (1986), 615–630.
30. B. J. Lucier, *A moving mesh numerical method for hyperbolic conservation laws*, Math. Comp. **46** (1986), 59-69.
31. ——, *Regularity through approximation for scalar conservation laws*, IMA Preprint # 336 (1987).
32. S. Osher, *Convergence of generalized MUSCL schemes*, SIAM J. Numer. Anal. **22** (1984), 947–961.
33. S. Osher and S. Chakravarthy, *High resolution schemes and the entropy condition*, SIAM J. Numer. Anal. **21** (1984), 955–984.
34. R. Sanders, *A third-order accurate variation nonexpansive difference scheme for single nonlinear conservation laws*, Math. Comp. **51** (1988), 535–558.
35. C.-W. Shu, *TVB uniformly high-order schemes for conservation laws*, Math. of Comp. **49** (1987), 105–121.
36. ——, *TVB boundary treatment for numerical solutions of conservation laws*, Math. Comp. **49** (1987), 123–134.
37. ——, *TVD time discretizations*, SIAM J. Sci. Statist. Comput. **9** (1988), 1073–1084.
38. C.-W. Shu and S. Osher, *Efficient implementation of essentially non-oscillatory shock-capturing schemes*, J. Comput. Phys. **77** (1988), 439–471.
39. ——, *Efficient implementation of essentially non-oscillatory shock-capturing schemes,* II, J. Comput. Phys. **83** (1989), 32–78.
40. P. Sweby, *High resolution schemes using flux limiters for hyperbolic conservation laws*, SIAM J. Numer. Anal. **21** (1984), 995–1011.
41. C. Tong and Z. Yu-Xi, *Two dimensional Riemann problems for a single conservation law*, Institute of Mathematics, Academia Sinica, Preprint # 20 (1985).
42. C. Tong and C. Guiquiang, *Some fundamental concepts about systems of two spatial dimensional conservation laws*, Acta Math. Sci. **6** (1986), 463–474.
43. D. Wagner, *The Riemann problem in two space dimensions for a single conservation law*, SIAM J. Math. Anal. **14** (1983), 534-559.

SCHOOL OF MATHEMATICS, UNIVERSITY OF MINNESOTA, MINNEAPOLIS, MINNESOTA 55455.
E-mail: cockburn@csfsa.cs.umn.edu

DIVISION OF APPLIED MATHEMATICS, BROWN UNIVERSITY, PROVIDENCE, RHODE ISLAND 02912
E-mail: am508000@brownvm.bitnet